THE PROCESS OF FUEL TRANSPORT IN ENGINE OIL

by

Norman Peralta

Bachelor of Science in Mechanical Engineering
University of Michigan
(1995)

Submitted to the Department of Mechanical Engineering
in Partial Fulfillment of the Requirements for the Degree of

Master of Science in Mechanical Engineering

at the

Massachusetts Institute of Technology; May 1997

Signature of Author_____
Department of Mechanical Engineering

Certified by_____
Simone Hochgreb
Associate Professor, Department of Mechanical Engineering
Thesis Supervisor

Accepted by_____
Ain A. Sonin, Chairman
Departmental Committee on Graduate Studies
Department of Mechanical Engineering

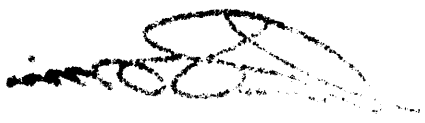

THE PROCESS OF FUEL TRANSPORT IN ENGINE OIL

by

Norman Peralta

Submitted to the Department of Mechanical Engineering on May 26, 1997
in partial fulfillment of the requirements for the Degree of Master of Science
in Mechanical Engineering.

ABSTRACT

An experimental method was developed which enabled sampling of oil from the piston skirt and sump of a firing spark-ignition engine. Fuel species in engine oil from both locations were quantified during cold start and steady state conditions using an adapted gas chromatography method. For engine warm-up at a part-load, low speed condition, the profile of liner oil fuel concentration during warm-up had a similar time constant to the calculated liner oil temperature. During warm-up and into steady state, the concentration of fuel in the sump began exceeding that in the liner oil at a crossover point which occurred at later times for heavier fuel species. Heavy hydrocarbons are preferentially absorbed in the liner and sump oil. At steady state, a strong correlation was observed between the mass fraction of fuel species absorbed and their individual boiling points, in both the liner and sump oil.

The oil sampling data, along with crankcase gas and blow-by sampling were inputs to fuel transport model. The liner oil refreshment rate and the fraction of fuel in blow-by were estimated as model parameters from experimental data. Conservation of the mass of fuel species in the liner and sump oil was used to determine the direction and magnitude of species mass fluxes between the sump and liner oil, and the crankcase gases. For the test fuel and individual fuel species modeled, a mass flux from the crankcase gas to the sump oil was calculated. This flux generally increased from warm-up until steady state concentrations in the sump and liner oil were reached. From calculations involving the liner oil control volume, it was determined that during engine warm-up there is a net flux of fuel species to the liner oil from cylinder gas, crankcase gas and blow-by gas fuel species. The direction of this net mass flux reverses at the point when the concentration of fuel in the liner oil is equal to that in the sump oil.

Thesis Supervisor: Simone Hochgreb
Title: Associate Professor of Mechanical Engineering

ACKNOWLEDGEMENTS

During the course of a project, the desire to understand a particular phenomenon pushes researchers to examine it very intently. One thing I was not expecting to discover in my two years as a research assistant was the tremendous generosity of people in helping me achieve the goals of this project. The Sloan Automotive Laboratory is blessed with faculty who possess a deep understanding of science, and the ability to share that with others. Professor Simone Hochgreb kept this project clearly focused, and consistently challenged me to improve my technical abilities. I am grateful for her insight and the opportunity to work on this project. Professors Cheng and Heywood also were very accessible, and cast illuminating perspectives on several aspects of this study.

A group of people made a very large impact on this project. Vincent Frottier of PSA was a superb colleague and friend. He provided expert instruction on the art of GC oil analysis, lessons in engine assembly and clearly introduced all phases of this project. J.R. Linna of the Sloan Automotive Laboratory and Kent Froelund from the Technical University of Denmark also made significant contributions to this work. J.R. provided fuel solubility data, and also donated a fine pair of used Rollerblades. Kent Froelund had many helpful suggestions and was always available for friendly chats about current research. Tian Tian, Steve Casey, and Denis Artzner all assisted with lubrication information.

I am indebted to Paul Harvath at the GM Chemistry Labs for teaching me how to think like a chemical analyst. In the engine cell, Haissam Haidar patiently spent long hours assisting with the Saturn, Mark Kiesel made excellent suggestions during hardware difficulties, and could double as a crack OSHA regulator. Peter Menard and Brian Corkum were absolutely indispensable, and saved hours of time through insightful suggestions. David Kayes was very helpful in understanding GC analysis of gas samples and the flammability of fuel in engine exhaust pipes. My friends in the Sloan Lab made the two years at MIT very rewarding. Brad Vanderwege, Mike Shelby, Robert 'cool directly' Meyer, Mark Dawson, Carlos 'Cadillac' Herrera, Ertan Yilmaz, Younggy Shin, Samgyeong 'Daewoo' Han, and Kelly M. Baker were tremendous officemates. I would like to thank Dr. B.J. Lim for his friendship and excellent taste in Asian cuisine. Nancy Cook, Wolf Bauer, Pierre Mulgrave, Marcus Stewart and Alan Shihadeh all were a pleasure to interact with.

Most importantly, I want to thank my family for the support, understanding and love they have provided throughout my life. Maria Zamora, who is an ace chemical engineer, my best friend, and my fiancee, will always have my admiration and gratitude for filling my life with happiness.

Norman Peralta
26 May 1997

TABLE OF CONTENTS

LIST OF FIGURES

LIST OF TABLES

ABBREVIATIONS

SYMBOL	DEFINITION	UNITS
A_i	area of species on sample chromatogram	-
A_{ref}	area of reference peak on sample chromatogram	-
B	cylinder bore	-
d	piston ring groove depth	m
D	piston diameter	m
f_{ch}	mass fraction of charge in blow-by gas	-
f_r	mass fraction of residual gas	-
h	height of piston ring groove	m
H_i	Henry's constant	kPa
H_i^*	non-dimensional Henry's constant	-
l	length of a particular liner region	m
$\dot{m}_{\mathrm{abs}_i}$	liner species mass fluxes from absorption and desorption of species in cylinder gases, oil consumption, and liquid fuel impingement	kg/s
$\dot{m}_{\mathrm{inj}_i}$	rate of fuel species injection during stoichiometric engine operation	kg/s
$\dot{m}_{LC_i}$	fuel species mass flux between liner oil and both crankcase gas and blow-by gas	kg/s
$\dot{m}_{\mathrm{net}_i}$	net mass flux of fuel species absorbed in the liner oil (non-oil transport)	kg/s
$\dot{m}_{\mathrm{oil}}$	mass flow rate of oil between the sump and liner	kg/s
$\dot{m}_{\mathrm{PCV}_i}$	fuel species mass flux between the crankcase gas and the positive crankcase ventilation valve	kg/s
$\dot{m}_{SC\,i}$	fuel species mass flux between crankcase gas and sump oil	kg/s
M_L	mass of oil on the liner	kg
M_S	mass of oil in the sump	kg
N	engine speed	rpm
P_e	brake mean effective pressure	bar
p_i	partial pressure of fuel species in gas phase	kPa
R	cylinder oil refreshment rate	-
T_{BC}	temperature of the liner at bottom center	°C

SYMBOL	DEFINITION	UNITS
T_{LO}	average temperature of the liner oil	°C
T_{TC}	temperature of the liner at top center	°C
V_i	volume of oil in a ring groove	m^3
x_i	mole fraction of fuel species in oil	-
X_i	mass fraction of fuel species in oil	-
X_{ref}	mass fraction of a reference standard in GC analysis	-
$X^{b}_{CO_2}$	mass fraction of CO_2 in burned cylinder gas	-
$X^{ch}_{CO_2}$	mass fraction of CO_2 in charge	-
$X^{cyl}_{CO_2}$	mass fraction of CO_2 in cylinder gas	-
δ	oil film thickness	m^3
ε	fractional uncertainty	-
φ	flooded fraction of ring groove volume	-

CHAPTER 1

INTRODUCTION

1.1 Background

The purpose of reducing hydrocarbon emissions from automotive engines is to avoid the negative health and atmospheric effects that result when hydrocarbons are released into the atmosphere. Reactive hydrocarbons and nitric oxides in the troposphere combine in the presence of sunlight to form ozone. Ozone is a lung and eye irritant and damages crops. Ozone formation in many major cities is a visible result of unburned hydrocarbons being emitted from internal combustion engines. Hydrocarbons which escape complete combustion can be hazardous to humans; benzene and 1,3-butadiene are common fuel species which can be toxic at high levels. Finally, since fuel hydrocarbons are a source of chemical energy, their emission annually represents thousands of gallons of fuel which have not been productively used.

Engine manufacturers and researchers are addressing the hydrocarbon emission (HC) problem in internal combustion engines with vigor as a result of increasingly strict global emissions regulations. HC emissions have been reduced by a factor of three compared to 1972 levels [1]. Much of this reduction came as a result of the introduction of unleaded fuels. Unleaded fuel allows for closed loop engine control and effective catalyst exhaust gas after-treatment systems. Engine design measures, such as improvements in fuel metering, mixture formation, crankcase ventilation, valve timing, ignition systems and combustion chamber design have also contributed greatly to lowering HC emissions. Cheng *et al.* outlined a general framework identifying HC emission sources and their magnitudes [2]. While comprehensive, the framework only estimates the relative importance of HC sources at warmed-up conditions. Proposed emission levels of 0.13 g HC/mile in the United States Tier II regulations will require a deeper understanding of the mechanisms leading to HC emissions [3].

There are several mechanisms by which fuel escapes complete oxidation in the engine. Crevices in the combustion chamber (spark plug threads, spaces between the piston lands and cylinder wall, head gasket gaps, valve seat crevices) fill with charge during the intake and compression strokes. This fuel remains unburned as the flame passes the crevice entrance, and exits to the combustion chamber when the cylinder pressure decreases. Crevice sources and absorption processes occurring in combustion chamber deposits and oil layers together may account for 30-60% of the engine-out HC emissions at warmed-up conditions [4]. Flame quenching is the process by which the flame in the combustion chamber is extinguished near the cool cylinder walls. This leaves a layer of unburned fuel near the walls which either oxidizes later in the cycle or is carried into the exhaust port with the burned gases. The amount of quenching varies with

combustion systems but during steady operation is thought to account for 1-5% of engine-out HC emissions [2]. Engine misfires and incomplete valve closure are other less significant sources of HC emissions.

Under cold engine conditions, unvaporized liquid fuel is thought to contribute as much as 50% of the unburned HC leaving the engine [5,6]. Liquid fuel can build up in the intake port, particularly during a cold start, and then enter the cylinder along with air and the vaporized portion of the fuel. This liquid fuel burns less easily than vaporized fuel and may impinge on oil layers, or partially burn in pool fires. A fraction of the liquid fuel in the cylinder may also escape past the piston rings with the blow-by gases. Liquid fuel-related HC emissions have not been fully explained, but are of great interest because of their importance during cold start. Another area that has not been completely described is fuel interaction with oil layers. Oil layers on the engine liner absorb and desorb unburned fuel during engine operation. There is an unburned fuel concentration gradient between the fuel mixture and oil layers during the intake and compression strokes. The compression process forces unburned fuel into the oil layers on the liner and the cylinder head. Following peak pressure in the cylinder, the unburned fuel concentration gradient reverses and cylinder pressure decreases. This allows for diffusion of the unburned fuel back into the combustion chamber where a fraction of this fuel may exit as unburned hydrocarbons. The interaction of ring pack and sump oil with blow-by gases is less well characterized, but may possibly influence HC emissions in a similar manner. The fuel-rich crankcase gases interact with the lower segment of the liner, and may add or remove HC that participate in the absorption and desorption mechanism. The mass fluxes of hydrocarbons into and out of the engine oil, by means of the processes described above, are the focus of this project.

1.2 Previous Work

Most HC emission studies involving fuel interaction with lubricants have centered on the measurement and interpretation of HC emissions resulting from engine operation using different fuels or lubricants. By estimating the oxidation of fuel desorbed from oil layers and making exhaust gas HC measurements, researchers have been able to test models of the absorption and desorption process [7]. Norris' work showed that desorption of fuel species from the oil layer is limited not by the rate of diffusion, but by the amount of fuel absorbed into the oil [8]. Unfortunately, there are a number of complicating factors which make results from even well-controlled tests difficult to interpret. The processes involving the lubricant are a subset of the total absorption-desorption process. This subset may provide insight into the rate at which fuel enters or leaves the lubricant oil.

A number of researchers have characterized typical fuel concentration levels in engine oil for a variety of operating conditions. Schwartz measured fuel dilution in oil of up to 10% by mass during a cold start, short trip service study [9]. More typical levels at normal engine temperatures are 1-4% by mass. Murakami *et al.* observed increases of HC in oil for increasing fuel-air ratio and for increased load (0.04%

HC increase / N·m of torque increase) [10]. Furthermore, decreasing engine temperature resulted in increased HC emissions. These results support the view that fuel component solubility in oil, which is a function of temperature and pressure, controls the amount of fuel absorbed in oil. This work attempts to confirm the role of solubility in the fuel absorption process.

Researchers interested in oil degradation, varnish formation, and HC emissions have sampled and analyzed engine oil. The method by which oil samples from the engine are obtained is critical to how they can be used to interpret the processes occurring in different parts of the engine. Samples obtained from the sump oil alone do not provide a direct view of the processes occurring on the cylinder liner, as there are a number of opportunities for HC transport to and from the oil, and mixing before it reaches the sump. The most interesting, and more difficult location from which to sample is on the cylinder liner or in the piston ring pack. This has typically been accomplished by drilling a sampling hole in the piston and using a linkage to transport the oil sample out of the engine. Saville *et al.* used such a mechanism to sample oil from the liner at sampling rates from 2 to 20 mg/min. [11]. At low sampling rates, changes in oil properties occurring during warm-up cannot be detected. Murakami *et al.* sampled a mixture of oil and blow-by from the piston ring pack and condensed the sample, which may cloud some of the distinction between what HC are present in the blow-by and what are present in the oil [10]. Our current work aims to sample liner oil at a sufficiently high rate to give insight into the development of HC concentrations during engine warm-up.

This study is a continuation of work begun by Vincent Frottier of PSA [12]. The gas chromatographic method he helped develop to analyze fuel content in oil is used and documented here. A liner oil sampling system was also developed, and is used extensively in this study to provide liner oil samples. Frottier conducted steady state sump oil sampling which provided baseline data to compare with liner oil concentrations. A better understanding is needed of the complex processes in which fuel interacts with the engine oil. Absorption of cylinder gas, crankcase gas and blow-by gas are all processes by which vaporized fuel can enter the oil. Fuel can leave oil layers through transport between the sump and liner oil, vaporization, desorption and oil consumption. Liquid fuel interaction with liner oil layers is also possible. The intent of this work was to capture more fully the basic processes involving the oil, while building on the knowledge that has been developed.

1.3 Objectives

Previous work on HC transport in oil layers consists primarily of tests in which parameters such as engine conditions, temperatures, fuels and lubricants were varied to determine their effect on hydrocarbon emissions or fuel concentration in oil. In this work, the liner oil layers, sump oil, blow-by and crankcase

gases were sampled. Subsequent chemical analysis and modeling were undertaken to meet the following objectives:

1. Develop a framework for fuel-related hydrocarbon transport between the liner oil layers, sump oil, blow-by and crankcase gases.

2. Determine parameters (both fuel related and operating condition related) controlling the total amount of fuel transported to the oil.

CHAPTER 2

LINER OIL SAMPLING SYSTEM AND OIL ANALYSIS

A method was developed to obtain liner and sump oil samples from a firing, four-cylinder spark ignition engine. Upon collection, the samples were analyzed to determine their fuel content, and this information was used to understand controlling parameters for fuel absorption (Chapter 3) and as input to a fuel transport model (Chapter 5). There are a number of important considerations for both the hardware and procedure when sampling liner oil. The oil sampling hardware should not alter normal engine operation. For instance, use of heavy sampling lines or additional fasteners can change the effective mass of the connecting rod and piston, which may influence engine performance. The sampling system must be compact, since space available for sampling lines is very limited within the engine. Finally, the system should be easy to install and maintain, and have a safe failure mode in the high speeds, temperatures and pressures present in the engine. The procedure for sampling cylinder liner oil is subject to another set of requirements. The most important of these requirements are liner oil sampling rate and quantity. The sampling rate must be consistent with periods short enough to capture rapid changes in concentration without unnecessarily increasing analysis effort. The sampled quantity must be large enough to undergo multiple chemical analysis tests, yet not so large as to alter the lubrication process in the liner region.

2.1 Engine and Fuel Characteristics

A Saturn four-cylinder engine running on an engine dynamometer was used for all of the experiments described in this study. The performance characteristics of the engine are outlined in Appendix A. The torque produced during experiments was 25 N·m at an engine speed of 1600 rpm. The engine operated at stoichiometric air/fuel ratio under the engine computer control. The fuel used in the warm-up and steady state testing was Chevron reformulated gasoline FR1760, with the composition shown in Table 2.1. This fuel contains additives which encourage combustion chamber deposit growth, but do not contribute to intake deposit formation. This fuel was used because simultaneous deposit build-up tests were being conducted on the engine. Chevron provided a detailed GC analysis of the species in the fuel which aided in the analysis of oil samples . The engine oils used in testing were Fleetline SAE 5W-30 mineral oil (SG grade, API group III designation) and the SH grade of the same oil. The SG grade oil was used for both the warm-up and steady state tests described in Chapter 3. The SH grade oil was used for the test in (Section 3.1.2) which oil was sampled from the anti-thrust side of the piston skirt, and for fuel variation tests.

Table 2.1 Chevron FR1760 fuel composition

Chemical Class	Percent by Weight
Saturates	49.3
Olefins	9.0
Aromatics	3.15
Oxygenates (MTBE)	10.2 (9.69)

2.2 Liner and Sump Oil Sampling System

The liner oil sampling system consists of a series of carefully placed sample lines connected to a piston, and routed along existing engine hardware (Fig. 2.1). A 1 mm diameter hole was drilled through the piston skirt 0.5 mm below the oil control ring. The hole is located either on the thrust or anti-thrust side of the piston in cylinder 4 of the engine (Fig. 2.2). A stainless steel (1 mm ID) tube was press-fitted into the hole from the interior of the piston and then covered with a high temperature epoxy. A flexible, temperature resistant PTFE tube was connected to the stainless steel, and carefully looped to pick up slack from connecting rod rotation (see Fig. 2.3). This tubing was positioned in a recessed portion of the connecting rod and passed through a small hole drilled in the shoulder of the connecting rod bearing cap. The tubing was connected to a strong 0.762 mm ID PEEK tube which was looped around a rod placed in the sump. This connection was made with a temperature resistant epoxy. The tubing then exited the sump to a cassette displacement pump, which provided the pressure to set up a sampling flow. Sump oil was also sampled simultaneously by inserting the 0.762 mm ID tube part way into the oil pan. A description of the equipment and settings used in liner and sump oil sampling is contained in Appendix A.

A source of difficulty encountered using the sampling hardware was avoiding kinks in the tubing at location A (Fig. 2.3). This could be seen fairly easily once the piston was installed, by turning the crankshaft over by hand and observing the tubing in this location. A more serious and frequently occurring problem was breakage of the connection between the two types of tubing just beyond the bearing cap. This was the result of an incorrect amount of tubing looped around the rod placed in the sump. A failure of this sort would be detected at the start of oil sampling and was indicated by a much larger than expected flow of oil from the liner oil sampling line, since the sampling tubing would be lying within the sump oil. Once correctly installed, the system worked well, permitting long sampling runs with no failures during operation. As mentioned above, the sampling hole is located on the thrust side of the piston for some of the experiments and on the anti-thrust side of the piston for others. This location was chosen based on observations of the lubricant films in an engine with a quartz cylinder which showed that a large quantity of oil was present between the liner and the piston skirt. Originally, the sampling hole was drilled in location B (Fig. 2.3), but it was difficult to draw oil from that section of the piston. Attempts to sample oil from this location resulted in little oil and large amounts of blow-by gas.

2.3 Procedure

The test engine was instrumented to measure oil and coolant temperature, intake manifold average pressure, exhaust oxygen content and other basic engine parameters. Prior to each experimental run, the engine oil was flushed and the oil filter was replaced. The engine was motored for approximately ten seconds before starting under engine computer control. At this time, the cassette pump was activated and continuous sampling of oil from the liner and sump began. The cassette displacement pump was set at 75% of full output and the flow from the sampling tubes was regulated with flow restrictors. Restriction of the sump oil sampling flow is necessary since the cassette pump is set to a high pressure in order to overcome the resistance in the liner oil sampling tube and inertial forces on oil in the sampling tube. The liner oil sampling tube length is 406 mm, with a corresponding sample transit time of 4 minutes, 16 seconds at the stated cassette pump setting.

After the initial transit time, the oil was deposited into 1.5 ml sample vials which were replaced at short intervals (3-10 minutes). By adjusting for the sample transit time, it was possible to determine when a particular oil sample was drawn from the liner. Liner oil was sampled at an average flow rate of between 0.10 - 0.12 ml/min, which represents removal of 5% of the estimated mass of oil on the cylinder liner in one minute. In Chapter 3, the percentage of the liner oil mass refreshed each revolution is estimated to be 1.25%. A comparison of these values shows that it is unlikely that the lubrication of the liner was altered by the sampling method. The liner and piston were examined after the tests were completed, and no abnormal wear was observed.

2.4 Sample Analysis

Gas chromatography (GC) analysis of the oil samples was used to identify absorbed fuel species and determine the mass fraction of species in the samples. A number of detector choices are available for this type of GC analysis. Perhaps the most effective combination of detectors is a flame ionization detector (FID) and a mass spectrometer (MS). The detectors would have to be used in separate sample runs since each technique destroys the sample. Sample quantification, cost and complexity make MS difficult, yet it is a very effective technique for identifying different fuel species. A single FID detector was used in this study because of its availability, convenience and successful use in related analysis. The strength of the FID is the nearly proportional response of the detector to the number of carbon atoms in each species sample, making quantification relatively simple. Retention indices or calibration samples are needed to identify unknown fuel species when using the FID, which is time consuming but adequate for this work.

Although a number of analysis standards exist for determining the total fuel dilution in oil, one which provides for the speciation of fuel components in oil was not available. Frottier *et al.* adapted ASTM method D3525-93 to allow for speciation of fuel components in engine oil [12]. The selection of an appropriate analytical

column (J&W Scientific DB-1, 60 m length, 0.32 mm inner diameter, 1 μm film thickness) and method allowed for good separation of fuel species throughout the entire range of absorbed fuel. The same type of column was used in the Auto/Oil Air Quality Improvement Research Program to separate fuel species in gas emission samples. A pre-column is used between the inlet and the analytical column to protect the column phase from the heavy oil components. Sample disturbance from the pre-column was rare, and the analytical column quickly degrades if the pre-column is not used. An alternate method to preserve the column, which uses flow valves to back-flush the slow moving heavy oil components from the column was considered, but not used.

A 5890 Hewlett-Packard gas chromatograph with split/splitless injection was used for the sample analysis. A complete listing of the analysis method, flow rates, and cylinder gases used is included in Appendix B. Each sample run consists of a 78 minute program followed by a minimum 1 hour bake of the column at 300 °C to drive off heavy oil components. Program times could be shortened by using a shorter column and different phase, but the long analysis time is an acceptable trade-off for good fuel component speciation. Split injection is used in this analysis, with a split ratio of 10. When the oil sample enters the inlet, it is immediately vaporized and mixed with the carrier gas, and 1/10 of this mixture is sent to the column while the rest is vented out of the GC. This split ratio is higher than typical ratios due to the small amount of sample injected into the inlet (between 1 and 2 μl).

The mass of oil in the sample vials is weighed before analysis, and approximately 1% w/w tetradecane is added as an internal reference standard. Tetradecane was not present in the fuel, and has a retention time between that of the heaviest fuel components and the lightest oil components (Fig. 2.5). Only about 1.5 μl of sample is injected into the inlet port, which is heated to 200 °C. Inlet temperatures of 300 °C early in the study led to breakdown of some of the lighter oil components, which then appeared in the regions of the chromatogram corresponding to absorbed fuel species. The sample is drawn into a micro-syringe without leaving an air gap, and the 'hot needle' injection method is used [13]. The needle is placed in the GC inlet for three seconds, and then the plunger is fully depressed and the syringe is immediately removed from the inlet. This procedure was not susceptible to needle discrimination and produced good peak resolution. Correct sample introduction is critical for reproducible results. Since air in the needle volume contributes to the total volume injected into the inlet, errors of up to 50% in sample peak areas can occur if proper care is not taken during injection [14]. Automatic sample injectors reduce this error, but might not have worked well with the oil samples. Since the oil samples were relatively viscous, care was required when filling the micro-syringe.

Hewlett-Packard Chemstation software running on a Hewlett-Packard Vectra computer was used to produce a chromatogram for each sample run. As mentioned above, the FID response is nearly proportional to the number of carbon atoms in each species sample. The majority of the fuel species present in oil have 7 or more carbons, with carbon to hydrogen ratios ranging from 7/8 (toluene) to (10/22) decane. We can conclude with reasonable accuracy that the area underneath each peak is proportional to the ratio of the area of the compound(s) of interest and the

reference peak. Therefore, calibration of each of the fuel species was avoided, and the mass fraction of each species i in fuel was calculated as:

$$X_i = \frac{A_i}{A_{ref}} \frac{X_{ref}}{(1 - X_{ref})} \tag{2.1}$$

where A_{ref} is the area of the reference peak, A_i is the area of the species of interest, and X_{ref} is the mass fraction of the reference standard (tetradecane) in oil (Fig. 2.4). For analysis of individual compounds, a more accurate measurement would correct for the C/H ratio of the individual compounds [12]. For most of the species absorbed in oil, this correction factor is not significant, so the simplified expression in Eq. 2.1 is used.

In the sample analysis of this study, each sample was analyzed at least twice, and the average of the results reported as the mass fraction of fuel species in oil. When particular fuel species were quantified in the oil, peaks were identified both visually and using retention times. When examining the mass fractions of individual fuel species in a chromatogram, the automatic integration performed by Chemstation was displayed on the computer screen. If a particular integration was deemed inaccurate, the integration was performed using the manual integration option included in the software.

Retention times for absorbed fuel species were consistent for approximately one year of heavy analytical column use. Because a small portion of the sample column is cut each time the column is installed, the retention times of fuel species gradually grew shorter as the column length decreased. A good indicator of the condition of the analytical column is the baseline value of the FID signal. For the analysis method and column of this study, a baseline FID response of 15 (arbitrary units) or below was generally acceptable. When the baseline detector signal remained high, overnight baking at 300 °C was sometimes successful. If this action failed to reduce the baseline signal, a solvent rinse of the column usually removed lingering oil species. Finally, storage of the column using septa, proper grades of cylinder gas and adequate filtration can extend the life of analytical columns used in this type of analysis significantly.

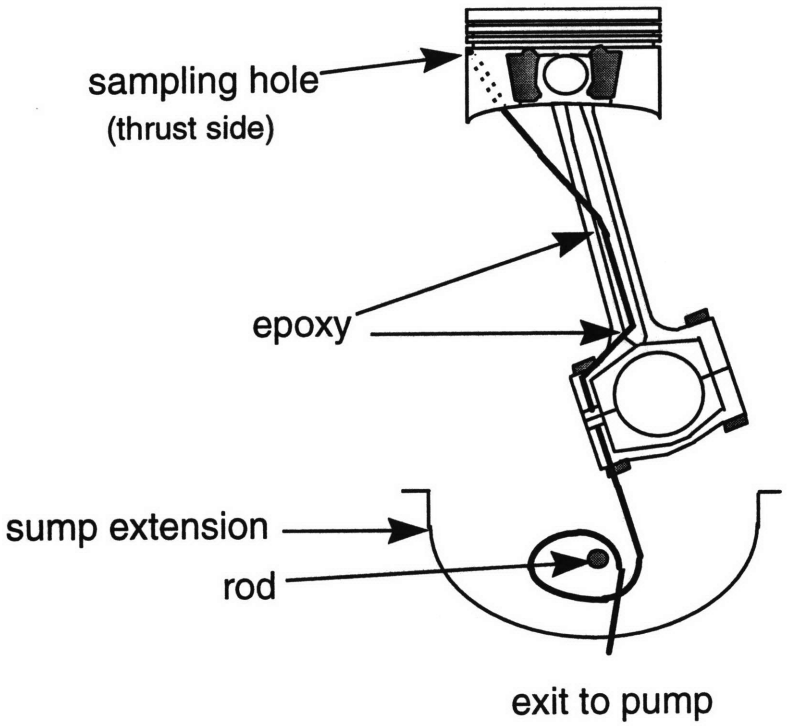

Fig. 2.1 Liner oil sampling system. *(Drawing adapted from [12])*

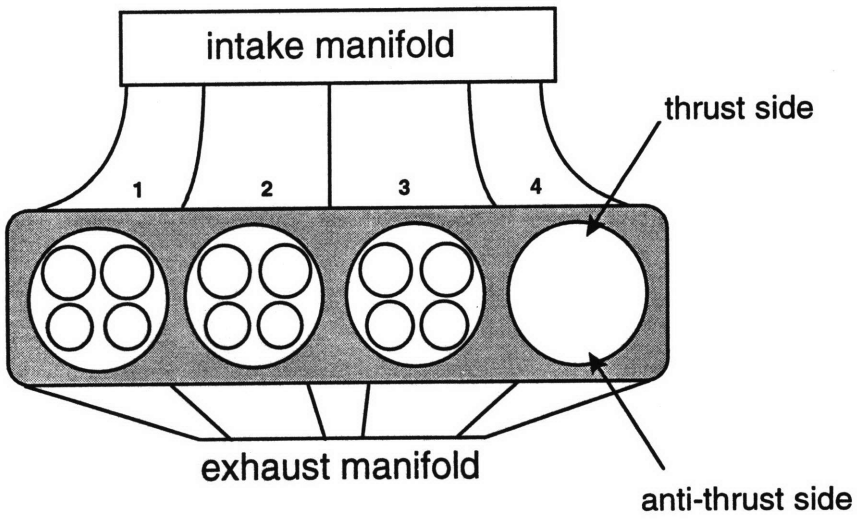

Fig. 2.2 Sampling location relative to engine block geometry. Arrows denote thrust and anti-thrust side piston skirt sampling locations.

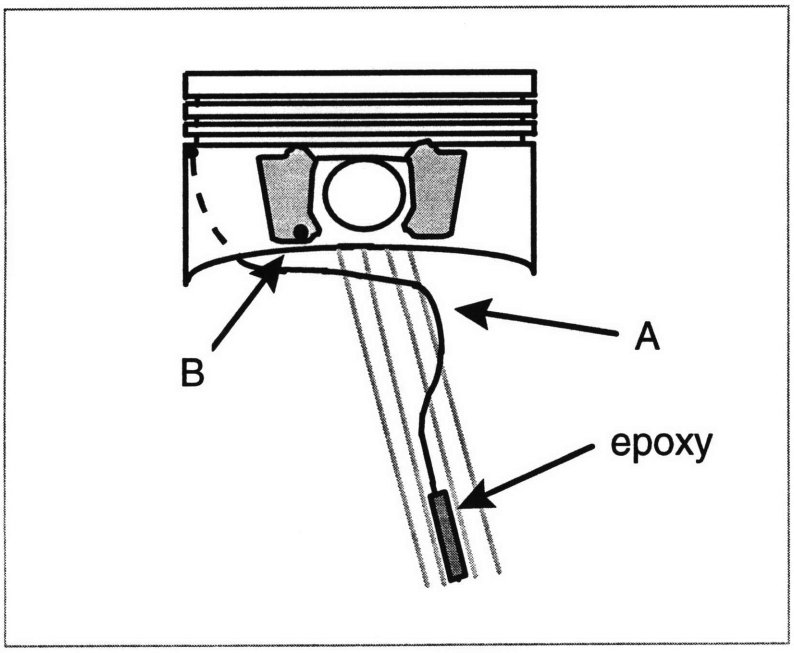

Fig. 2.3 View of the piston to connecting rod portion of the liner oil sampling system. Location A is the position where the sampling line would often kink, and B is the location of the original oil sampling hole.

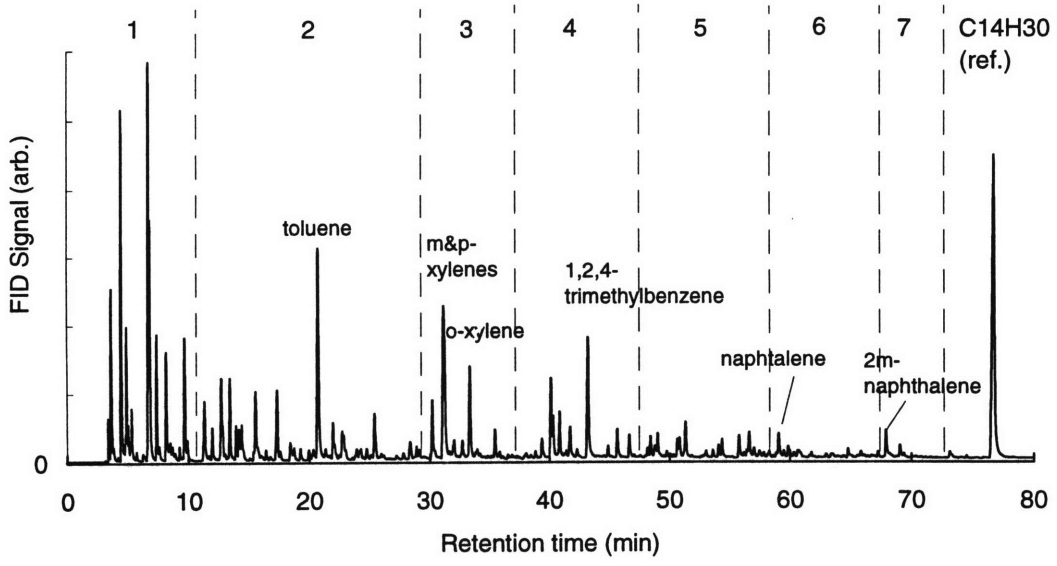

Fig. 2.4 Fuel chromatogram. Reference standard tetradecane visible at 78 minutes. Regions 1-7 are divisions of fuel species by retention time. *(Chart adapted from [12])*

CHAPTER 3

OIL SAMPLING EXPERIMENTS

In order to identify and quantify the fuel-related hydrocarbons in engine oil, a series of oil sampling experiments were conducted for low speed, low load engine conditions. The experiments vary in duration from twenty five minutes to three hours, and in sampling location (thrust and anti-thrust side of the piston skirt). Mass fractions of the total fuel absorbed in oil and individual fuel components absorbed are presented, along with analysis of the absorption characteristics of fuel in oil.

3.1 Engine Warm-up Tests

The engine was started from ambient conditions (25 °C) for the warm-up experiments and run for twenty seven minutes. Oil was sampled from the thrust side of the piston skirt in this experiment. The amount of fuel in each oil sample was expressed as the mass of fuel in the sample divided by the mass of the oil sample. The mass fraction of fuel present in oil sampled from the liner and from the sump is plotted in Fig. 3.1. The GC oil analysis shows that for the first ten minutes of engine operation, the mass fraction of fuel in the liner oil rises at a rate four times faster than that in the sump oil. After this time, the fraction of fuel in the liner oil rises less rapidly than its initial rate. The fraction of fuel in the sump oil increases at a consistent rate throughout the entire warm-up period. At the end of warm-up, the mass fraction of fuel in the liner oil is 0.41% and 0.29% in the sump oil. By integrating the mass fraction of fuel in the sump and liner oil, the net rate at which fuel accumulates in the engine oil can be determined. For the warm-up period, the net rate of fuel build-up in the sump oil is approximately 0.35 g/min, which is about 1.7% of the rate at which fuel is injected into the engine during stoichiometric operation. The liner oil has a lower fuel accumulation rate of approximately 0.2 mg/min. Although the fraction of fuel in the liner appears to level off at the end of the warm-up period, the test duration was too short to determine if a steady state had been reached at the conclusion of the test.

3.1.1 Fuel Species Absorption

Figure 3.2 shows the composition of fuel species in the liner and sump oil early in warm-up and at the conclusion of the test. Regions 1-7 correspond to fuel components grouped by increasing molecular weight. For analysis purposes, the chromatograms of oil samples were divided into seven regions based on the fuel species retention time. Some of the major fuel species included in each region are shown in the fuel chromatogram of Fig. 2.4. The distribution of fuel in both the sump and liner oil is skewed toward the heavy hydrocarbons compared to the original fuel. As the engine warms-up, the fraction of light fuel components in the liner oil decreases markedly. The fuel composition in the sump oil is nearly constant for

all regions except regions 1 and 2, which contain the lightest fuel components. Figure 3.3 shows that while the total fuel concentration in the liner and sump oil increases, the concentration of the major light fuel species (pentane, 2-methylbutane, Methyl Tertiary Butyl Ether (MTBE), and 2-methylhexane) does not increase from initial levels. In fact, at 27 minutes, these components have nearly reached a steady state concentration.

Some of the intermediate weight fuel species (7-9 carbon atoms) in the liner and sump oil are plotted in Fig. 3.4. Similarities in the build-up rate observed for light species are present for 2-methylhexane, toluene, xylene and 1,2,4-trimethylbenzene. One difference is that mass fractions of most of the intermediate weight fuel species in the liner and sump oil are 5 to 8 times as large as that of the lighter fuel species at the end of warm-up. A comparison of the relative amounts of these species in the fuel (Appendix B) indicates that this difference in build-up does not scale with the relative amount of each species in the fuel. Also, unlike the sump oil concentrations of the lighter fuel species, the intermediate weight fuel species are increasing steadily in the sump oil. The intermediate weight fuel species concentrations in the liner oil appear to be at a steady state after 27 minutes. The mass fraction in oil of two heavy fuel species (10-11 carbons) is shown in Fig. 3.5. Both heavy species have similar sump and liner oil concentrations throughout warm-up. During warm-up, the average rate of 2-methylnaphthalene and naphthalene build-up in the liner oil is nearly twice as fast as in the sump. The consistent increase of these heavy species in the liner oil differs from the rate of increase of the lighter species.

In Fig. 3.6, the liner and sump oil mass fractions of toluene are plotted together. After approximately 20 minutes, the mass fraction of toluene in the sump oil begins to exceed the fraction of toluene in the liner oil. The fact that the sump oil species concentration can exceed the liner oil species concentration indicates that there is another source of the particular species to the sump oil. However, it is also possible that fuel is quickly desorbing from the liner after being splashed up from the sump. In Fig. 3.3, the mass fractions of 2-methylpentane and MTBE in the liner oil also overtake the sump mass fractions early in warm-up. The time necessary for more fuel to accumulate in the sump than in the liner oil is related to molecular weight. Heavier fuel species such as the 2-methylnaphthalene, naphthalene and 1,2,4-trimethylbenzene are present in higher fractions in the liner oil than in the sump oil during warm-up (Figs. 3.4-3.5).

3.1.2 Anti-thrust Side Sampling Location

In order to determine how fuel concentration varies along the circumference of the liner oil, a warm-up experiment was conducted in which oil was drawn from the anti-thrust side of the piston skirt. The operating conditions and fuel were the same as for the thrust side warm-up test, except that the SH

grade of engine oil was used in the anti-thrust side test. As shown in Fig. 2.2, the sampling location in this test is on the exhaust side of the piston skirt, directly opposite of the intake-side location of the previous test. Depending on the injector spray characteristics and cylinder air motion, the amount of liquid fuel which impinges on the exhaust side of the cylinder may be different than on the intake side. This specific sampling location was chosen because it was likely that there would be sufficient oil to sample, and because the location of the sampling line did not have to be altered on the connecting rod. The only modification to the liner oil sampling system was a new piston with a hole drilled in the appropriate location.

Fig 3.7 shows a comparison between the fuel mass fraction in the liner oil during warm-up for both sampling locations. For the first 5-7 minutes of engine operation the mass fraction of fuel in the liner oil is identical for both locations. From 10 minutes until the conclusion of the test, the oil sampled from the anti-thrust side of the piston skirt had approximately 20% less absorbed fuel than the thrust side. Likewise, the fuel mass fraction in the sump oil during the anti-thrust test was approximately 25% less than in the thrust-side test. It is uncertain why the sump and liner oil concentrations in this particular test were lower, since engine temperatures were nearly identical to the previous warm-up test. One possibility for the difference in fuel absorbed is the slight difference in oils used in each test. Regardless of the difference in oil specification, relative to the sump oil fuel concentration, the concentration of fuel in the liner oil for both sampling locations is nearly identical. Analysis of the oil samples from the anti-thrust test showed that the composition of fuel species in both sampling locations was also very similar.

3.2 Three Hour Oil Sampling

There were several objectives to conducting a longer duration oil sampling test. One objective was to determine the liner and sump oil fuel species concentrations as they approached steady state. It was also of interest to determine if the crossover points discussed in Section 3.1 occur for all fuel species. Finally, concentration data from longer test runs show how fuel is absorbed and transported within the oil at constant temperature. The conditions and parameters of the three-hour oil sampling test were identical to the thrust side warm-up test in Section 3.1, except the engine operated for a longer, three hour time interval. During this test, oil was sampled from the thrust side of the piston skirt, as in Section 3.1.1. The final coolant and oil temperatures for the three hour test were 89 °C, which is 9 °C higher than at the end of warm-up. The temperature profiles for both tests were identical for the warm-up period, with the 9 °C increase in temperature occurring over 155 minutes. The effect of oil and coolant temperatures on fuel build-up is discussed in Section 3.3.

The mass fraction of fuel in the liner and sump oil for the three hour test is plotted in Fig. 3.8. In this test, the fuel mass fraction in the sump oil after three hours is 1.04%, compared to 0.78% in the liner

oil. After approximately seventy minutes of engine operation, the mass fraction of fuel in sump begins to exceed the mass fraction of fuel in the liner oil. The increase of fuel in the sump oil is nearly constant, with a slight decrease in the fuel build-up occurring after 90 minutes. The average rate of fuel accumulation in the sump oil between 25 minutes and 90 minutes is almost 0.3 g/min, which is slightly lower than the rate of fuel build-up in the sump oil during warm-up. A steady state concentration of fuel in the liner is reached after 120 minutes of operation (Fig. 3.8). After the warm-up period of 25 minutes, the mass fraction of fuel in the liner oil increases at an average rate which is three times lower than during warm-up.

The mass fraction of fuel in the sump and liner oil is separated into contributions by region in Fig. 3.9. In region 1, which includes fuel species such as pentane and hexane, the mass fraction of fuel species in the liner oil decreases with time. Regions 2 and 3, which contain fuel species such as toluene and xylene, have a nearly constant concentration in the liner oil following warm-up. Figure 3.9 shows that the mass fraction of heavy fuel species (regions 4-7) continues to increase in the liner oil until 120 minutes, when fuel concentrations in the liner oil reach steady state. Fuel-build up characteristics vary between the liner oil and sump oil. Heavy fuel species increase in the sump oil, but unlike the liner oil, a steady state is not reached (Fig. 3.9). Another difference in fuel build-up between the liner and sump oil is that the concentration of the lightest fuel species decrease in the liner oil, and do not in the sump. This is probably due to the lower temperature of the sump oil compared to the liner oil, which decreases the possibility of light fuel species vaporizing out of the oil.

Plots of the mass fractions of fuel species in the liner and sump oil are shown in Figs. 3.10-3.13. Toluene (Fig. 3.10) exhibits the build-up characteristics seen in regions 1 and 2 of Fig. 3.9. In Figs. 3.11-3.12, xylene and 1,2,4-trimethylbenzene both show crossover points as observed in the lighter species during warm-up. The mass fraction of 1,2,4-trimethylbenzene in the sump oil exceeds that in the liner oil at approximately 150 minutes, and for the lighter xylene, this occurs at 90 minutes. The build-up characteristics of 2-methylnaphthalene are shown in Fig. 3.13. The concentration of 2-methylnaphthalene in sump oil increases at nearly a constant rate during the three hour test. After three hours of continuous engine operation, 1.34 g of 2-methylnaphthalene is present in the sump oil. This is 4.4% of the total 2-methylnaphthalene injected during stoichiometric operation.

3.3 Data Analysis

In the oil sampling experiments described in this chapter, the molecular weight of fuel species was a distinguishing property of each fuel species which influenced the magnitude of fuel absorbed and the crossover time. Since molecular weight is also related to fuel species boiling point (Fig. 3.14), the engine

temperature and fuel volatility effects on fuel build-up are also analyzed in this section. Solubility of fuel species in oil is compared to oil sampling experiment data.

3.3.1 Effect of Temperature

K-type thermocouples in the sump oil pan and engine coolant outlet were used to monitor oil and coolant temperature during testing. The measured engine coolant and sump oil temperatures for the warm-up test are shown in Fig. 3.15. Comparing the mass fraction of absorbed fuel in the liner oil (Fig. 3.1) with the coolant temperature, it is evident that both change at a similar rate. The test engine was not instrumented with cylinder thermocouples to measure the oil temperature on the liner. Although the temperatures of the sump oil and engine coolant are nearly equal at the end of warm-up, liner oil temperature and sump oil temperature are much different. Correlations have been developed which estimate the liner temperature of a uniformly cooled single cylinder engine from coolant temperature and operating data. The liner temperature in siamesed bore multi-cylinder engines like the Saturn test engine is typically higher than in single cylinder engines due to less water jacket coverage. However, for low load operation, the temperature difference is not as significant between the two types of engines, permitting the use of a correlation developed by Froelund and Linna for liner temperature [15]. The liner temperature at top center (TC) in degrees Celsius is estimated as

$$T_{TC} = 98 + 5.4 \cdot 10^{-3} \cdot p_e \cdot N \tag{3.1}$$

where p_e is the brake mean effective pressure (bar) and N is the engine speed (rpm). The liner temperature at bottom center (T_{BC}) can be estimated as the measured engine coolant temperature. The average liner oil temperature (T_{LO}) can be estimated as the average of the liner temperature at top center and bottom center

$$T_{LO} = \frac{T_{TC} + T_{BC}}{2} \tag{3.2}$$

where the result is in degrees Celsius. The coolant temperature measured during engine warm-up, and the brake mean effective pressure at engine operating conditions are used in Eqs. 3.1 and 3.2. The calculated liner temperature, which is very close to the temperature of the liner oil, has a sharp rise for the first five minutes, and then increases 5-10 degrees over the next 20 minutes (Fig. 3.16). The mass fraction of fuel in the liner during warm-up (Fig. 3.1) shows nearly the same type of profile, except the rise in absorbed fuel occurs over ten minutes, not five. As discussed in Section 3.2, the sump oil is at a lower temperature than the liner oil, and this temperature difference might explain the lower concentration of light fuel species in the liner oil compared to the sump oil. This difference in fuel build-up rates of lighter species between the

sump and liner oil is seen in Fig. 3.2, where the light fuel species are a larger fraction of the fuel in the sump oil. The temperature difference between the sump and liner oil is as high as 50 °C during the first minute of warm-up, and falls to approximately 10 °C at steady state. This temperature difference might lead to less vaporization of the sump fuel species, or affect the temperature dependent solubility process.

3.3.2 Solubility

The characteristics of fuel solubility in oil are examined in this section. The solubility of fuel in oil is often described by an equation of the form:

$$p_i = H_i Y_i \tag{3.3}$$

where p_i is the partial pressure of the fuel species in the gas phase, Y_i is the mole fraction of the fuel species in the oil, and H_i is the Henry's constant of the particular species. H_i is a temperature dependent inverse solubility parameter which is determined by experiment. Equation 3.3 is only valid for small concentrations of fuel in the oil, which holds for the concentrations measured in this study. An alternate form of Eq. 3.3 is obtained by multiplying H by the ratio of the oil and fuel molecular weights. The resulting solubility parameter is H^*, which has units of pressure. The controlling law for solubility becomes

$$p_i = H_i^* X_i \tag{3.4}$$

where X_i is the mass fraction of fuel in oil. If Eq. 3.4 holds, engine oil at different temperatures will absorb different amounts of fuel, since H_i^* is temperature dependent. The oil in the liner and sump is exposed to different thermal conditions which results in a temperature difference of 20 degrees between the warmer liner oil and the sump oil at the end of engine warm-up (Fig. 3.16). Using the concentration measurements made in the crankcase gas and in the sump oil (Chapter 4), the partial pressure of several fuel species in the gas phase was compared to the corresponding concentration of fuel in the sump oil for up to 60 minutes, using Eq. 3.4. The results from the calculations showed that the measured concentrations of fuel species in the crankcase gas were substantially lower (10%-50%) than the equilibrium concentrations predicted by Eq. 3.4. Since there may have been sampling losses of the crankcase gas, it was difficult to draw firm conclusions from those calculations.

3.3.3 Fuel Species Boiling Point

In this section, measurements of fuel absorbed in the sump oil of the Saturn engine are analyzed. During these tests, the mass fraction of fuel in the sump oil reached a steady state of 1.35% after fifteen hours. The fuel and oil used in this steady-state experiment are identical to those used in the thrust-side warm-up tests of Section 3.1. The engine operating conditions were slightly different than in the tests described previously. An alternating cycle was used where the engine operated for 6 minutes at 1400 rpm/16.5 N·m, and 6 minutes at 2200 rpm/49.5 N·m. The purpose of this analysis is to compare the steady state species concentrations in the sump oil with steady state concentrations in the liner oil from the three hour test.

In order to determine the effect of temperature on fuel build-up in oil, the mass fraction of fuel species in the sump oil at 11 hours was compared to fuel species boiling points. In Fig. 3.17, the vertical axis is the ratio of the mass fraction of species (relative to total fuel hydrocarbon) in the sump oil relative to the mass fraction of the species in the fuel. The horizontal axis is the reciprocal boiling point of each species multiplied by 1000. There is a strong correlation between the mass fraction of fuel species in the sump oil and the individual boiling points. This correlation indicates that for increasing fuel species volatility, there is a decreasing amount of the fuel species absorbed in the oil. The mass fractions of fuel species in the liner oil can be plotted in the same manner. In Fig. 3.18, fuel species are plotted using mass fractions in liner oil from the three hour sampling experiment of Section 3.2. The same relationship of increased fuel absorption for species with high boiling points is observed. A line drawn though the points on both plots indicates similar slopes for both liner and sump data. The slope of the sump oil data in the semi-log plot (Fig. 3.17) is -2200 K and is -2400 K for the liner data in Fig. 3.18.

3.3.4 Fuel Variation Tests

The purpose of varying fuels was to distinguish between the effects of solubility and fuel volatility on fuel build-up in oil. Even though GC analysis allows for speciation of the Chevron fuel used in previous tests, distinct fuels can provide data which isolates specific species properties. Two specially blended research fuels provided by Exxon were used in warm-up tests in which oil was only sampled from the sump. One of the fuels tested was a fully-blended paraffinic fuel, and the other was a paraffinic fuel with 20% aromatic content. The Reid vapor pressure of the fuels was similar, as were the distillation curves. Because the fuels had comparable volatility, the presence of a significant fraction of aromatics in one fuel makes the solubility of fuel species in oil a differentiating factor. Generally, the solubility of aromatic fuel species in oil is higher than for paraffins.

The engine operating conditions in the fuel variation tests were identical to the warm-up test in Section 3.1. The lubricant used in these experiments was SAE 5W-30 mineral oil with the SH designation. As shown in Fig. 3.19, a higher mass fraction of the paraffinic-aromatic fuel was present in the sump oil during warm-up than the fully-blended paraffinic fuel. Gas chromatography analysis provided by Exxon of two oil samples at the end of warm-up also confirmed this result. The increased buildup of the more soluble fuel indicates that the effect of volatility in Section 3.3.3 may be separate from the influence of solubility in fuel build-up. If individual species of comparable volatility were identified with different solubility in oil, the measured mass fractions would clarify the role of solubility in fuel build-up. While the integrated results of the fuel variation tests suggest that solubility has a distinct effect from fuel volatility, it was not possible to identify fuel species in the test fuels which matched the above criteria. A complete analysis of the individual fuel species in both fuels was not available, so a detailed analysis of the absorption characteristics was not possible at this time.

3.4 Conclusions

In this chapter the accumulation of fuel species in the liner and sump oil of a four cylinder, spark-ignition engine was described for low load, low speed conditions. The engine was operated using a standard fuel of known composition and a commercial mineral oil. During the first ten minutes of warm-up, the mass fraction of fuel in the liner oil rises at a rate nearly four times faster than in the sump oil, with a build-up rate that matches the change in liner oil temperature. At the end of warm-up, the mass fraction of fuel in the liner oil is 0.41%, and 0.29% in the sump oil. For the warm-up period, the net rate of fuel build-up in the sump oil is about 1.7% of the rate at which fuel is injected into the engine during stoichiometric operation. After three hours of engine operation, the fuel mass fraction in the sump oil is 1.04%, compared to 0.78% in the liner oil. In this study, the point where the total fuel concentration in the sump oil exceeds the fuel concentration in the liner oil occurs at approximately 70 minutes of engine operation. This crossover point indicates that there is another source of fuel to the sump oil.

The distribution of fuel species in oil is skewed toward the heavy hydrocarbons, and the difference in absorption does not scale with the relative amount of each species in the fuel. Light fuel species reach the concentration crossover point between the liner and sump oil within the engine warm-up period, and also reach steady state during this time. Intermediate weight fuel species in the liner oil reach a steady state concentration within 100 minutes of operation and approach a steady state in the sump oil by the end of the three hour experiment. Heavy fuel species in the oil reach a steady state in the liner oil after 120 minutes but are still increasing in the sump after three hours. For the heaviest fuel species, up to 4.5% of the total amount injected is present in the sump oil after three hours. Relative to the sump oil fuel concentration, the concentration of fuel in liner oil on the thrust and anti-thrust sides of the piston skirt is nearly identical.

There is a strong correlation between the mass fraction of fuel species absorbed and individual boiling points, in both the liner and sump oil at steady state. The relationship between species absorption and boiling point was nearly identical in both the sump oil and the liner oil. This correlation indicates that for increasing fuel species volatility, there is a decreasing amount of the fuel species absorbed in engine oil. In a test with specially blended fuels of similar volatility, the sump oil mass fraction of the higher solubility fuel was approximately 25% greater than the sump oil mass fraction of the lower solubility fuel.

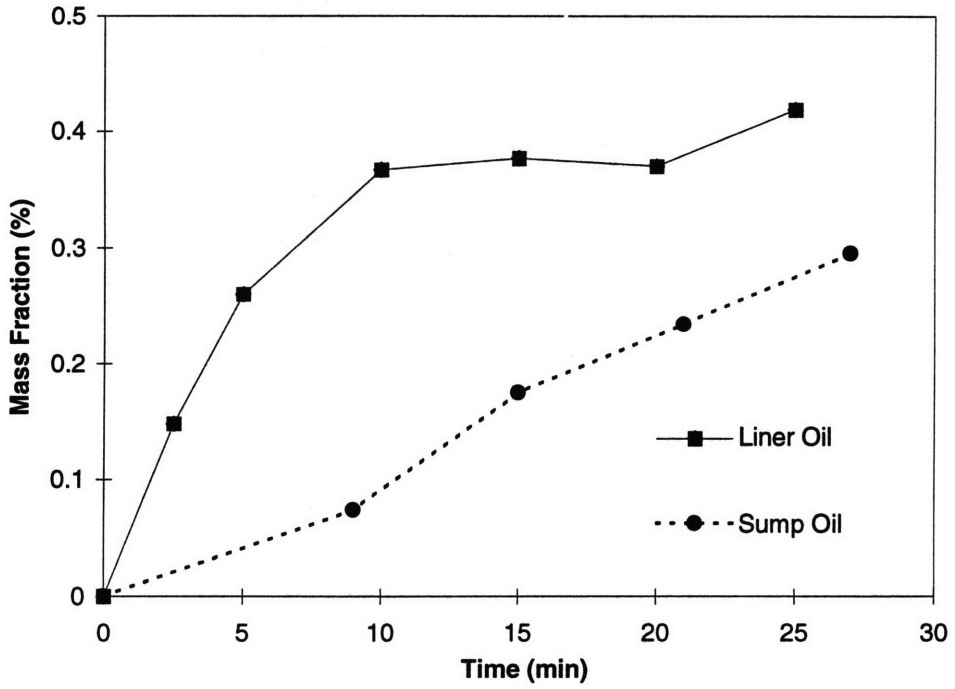

Fig 3.1 Total fuel mass fraction in liner oil and sump oil during engine warm-up. The oil sampling location was on the thrust-side of piston skirt.

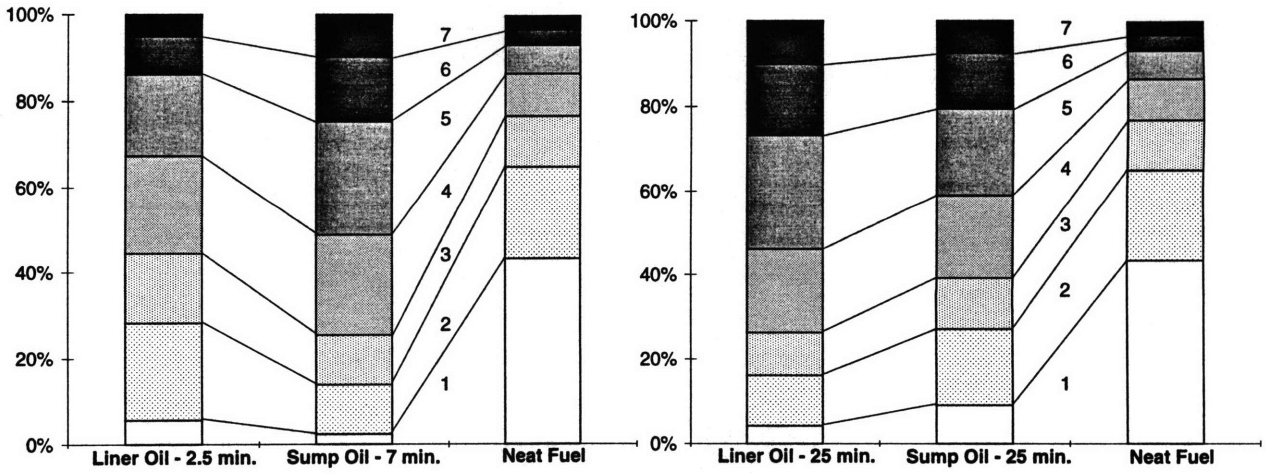

Fig. 3.2 Composition of the mass of fuel in the liner and sump oil during engine warm-up. Regions 1-7 correspond to fuel species in oil ordered by increasing molecular weight.

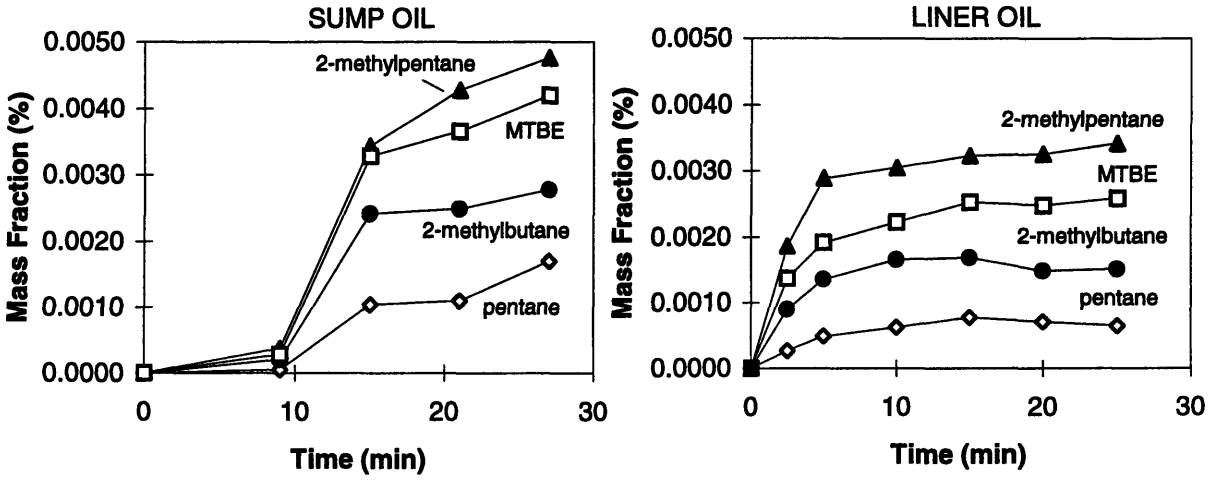

Fig. 3.3 Mass fraction of light fuel species in sump and liner oil during warm-up.

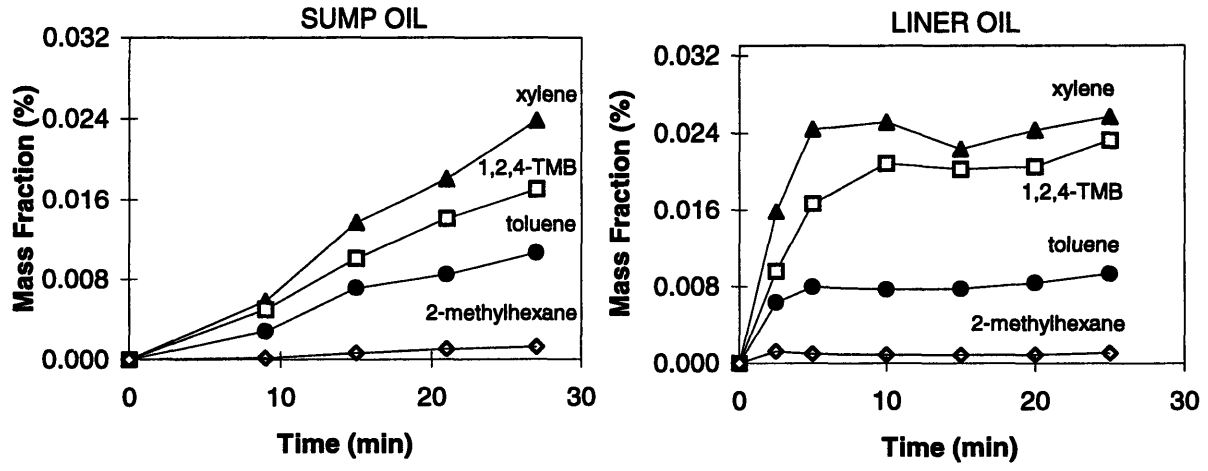

Fig. 3.4 Mass fraction of intermediate weight fuel species in the sump oil and liner oil during warm-up.

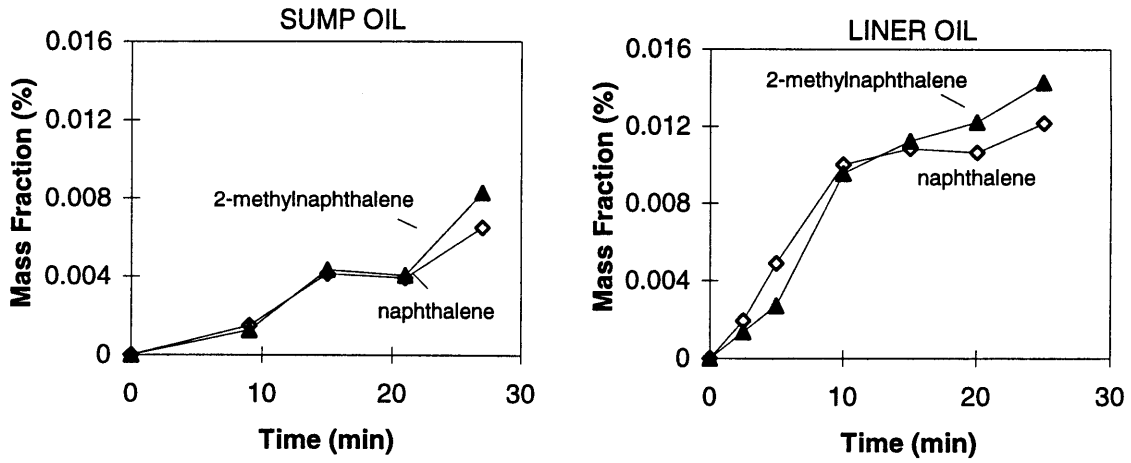

Fig. 3.5 Mass fraction of heavy fuel species in sump and liner oil during warm-up.

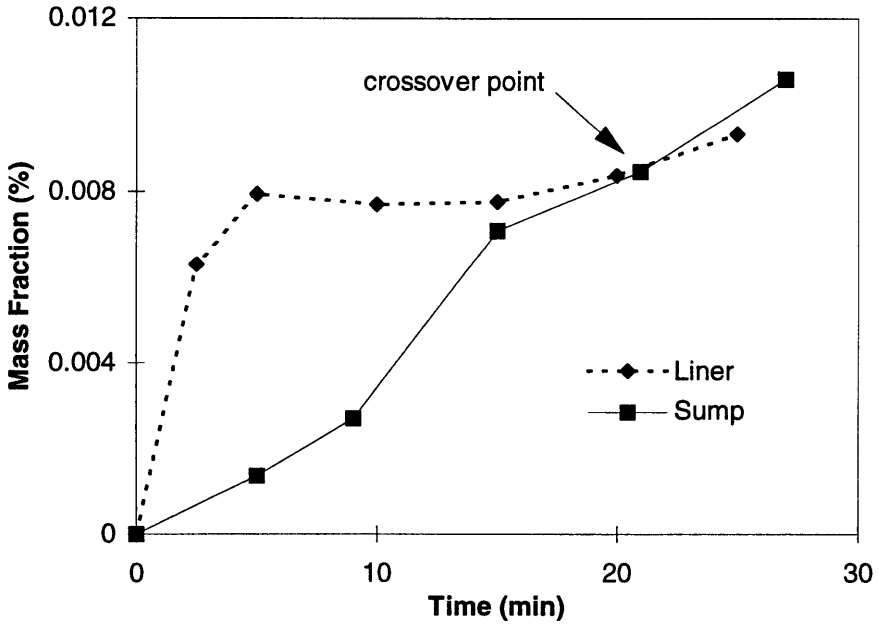

Fig. 3.6 Mass fraction of toluene in oil. Crossover point where sump oil toluene mass fraction exceeds mass fraction of toluene in liner oil occurs at 20 minutes.

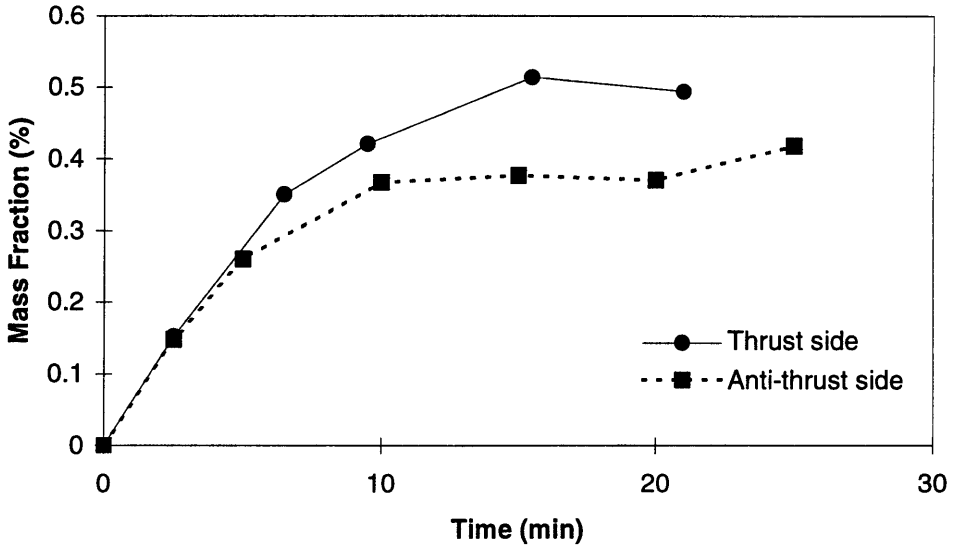

Fig. 3.7 Total fuel mass fraction in liner oil for warm-up oil sampling experiments. Oil sampling locations are from the thrust and anti-thrust side of the piston skirt.

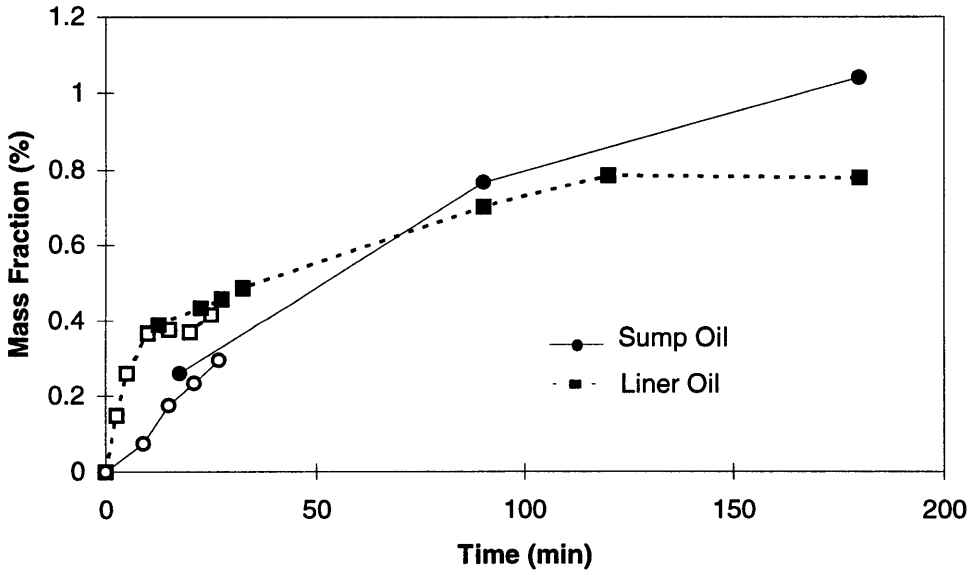

Fig. 3.8 Total fuel mass fraction in liner and sump oil for the 3 hour oil sampling experiment. Solid symbols are 3 hour test results. Open symbols are test results from the thrust side warm-up experiment plotted for comparison.

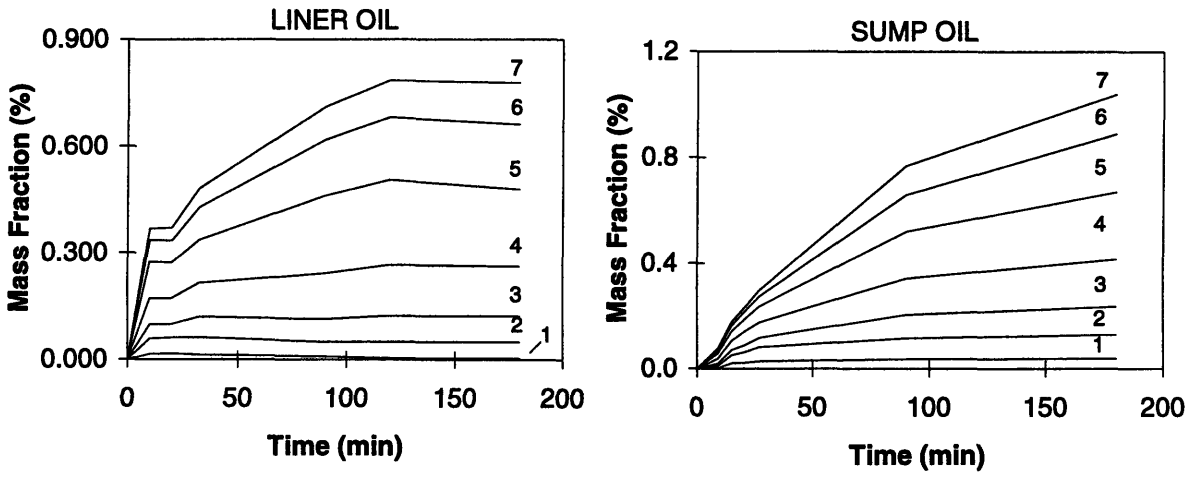

Fig. 3.9 Composition of the mass of fuel in liner and sump oil during 3 hour test. Regions 1-7 correspond to fuel species in oil ordered by molecular weight.

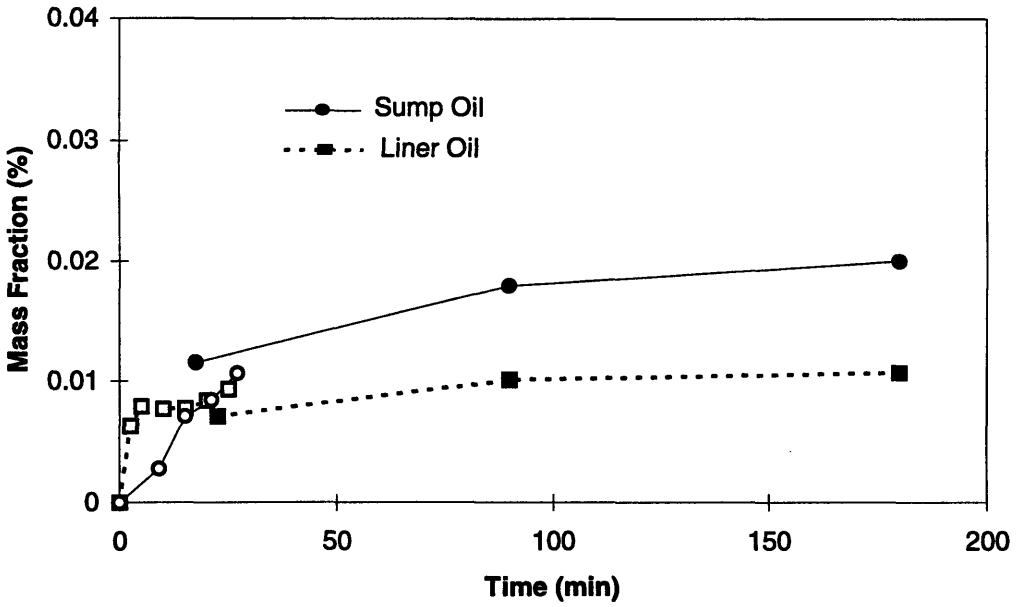

Fig. 3.10 Toluene mass fraction in liner and sump oil for the 3 hour oil sampling experiment. Solid symbols are 3 hour test results. Open symbols are test results from the thrust side warm-up experiment plotted for comparison.

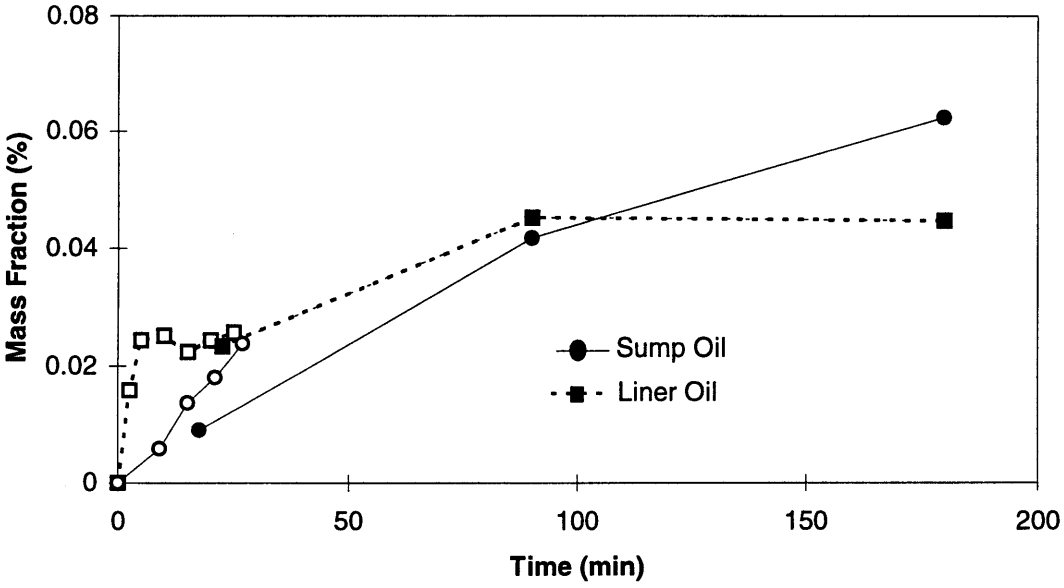

Fig. 3.11 Xylene mass fraction in liner and sump oil for the 3 hour oil sampling experiment. Solid symbols are 3 hour test results. Open symbols are test results from the thrust side warm-up experiment plotted for comparison.

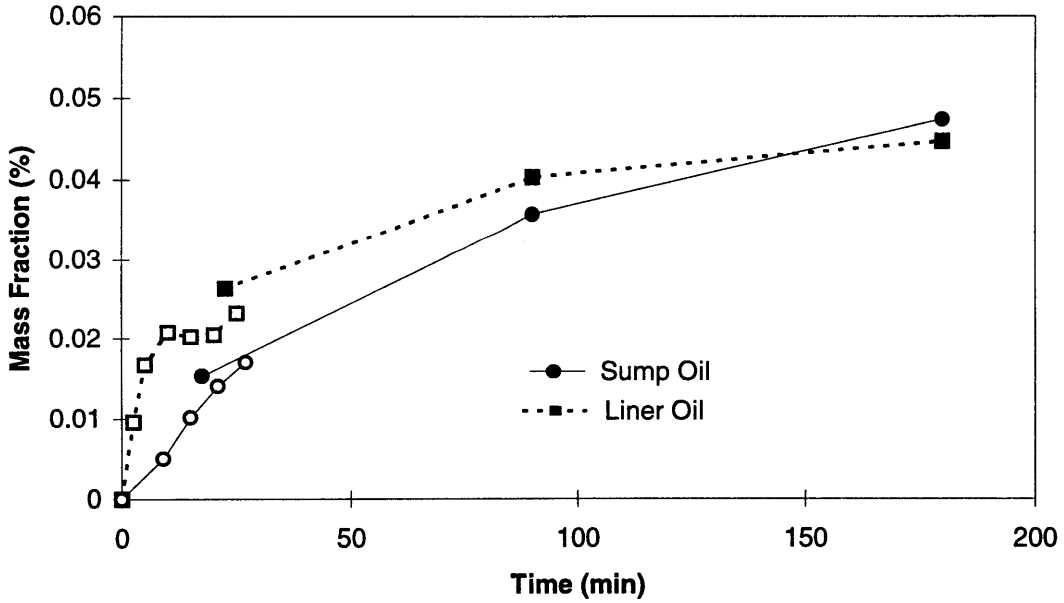

Fig. 3.12 1,2,4-trimethylbenzene mass fraction in liner and sump oil for the 3 hour oil sampling experiment. Open symbols are test results from the thrust side warm-up experiment plotted for comparison.

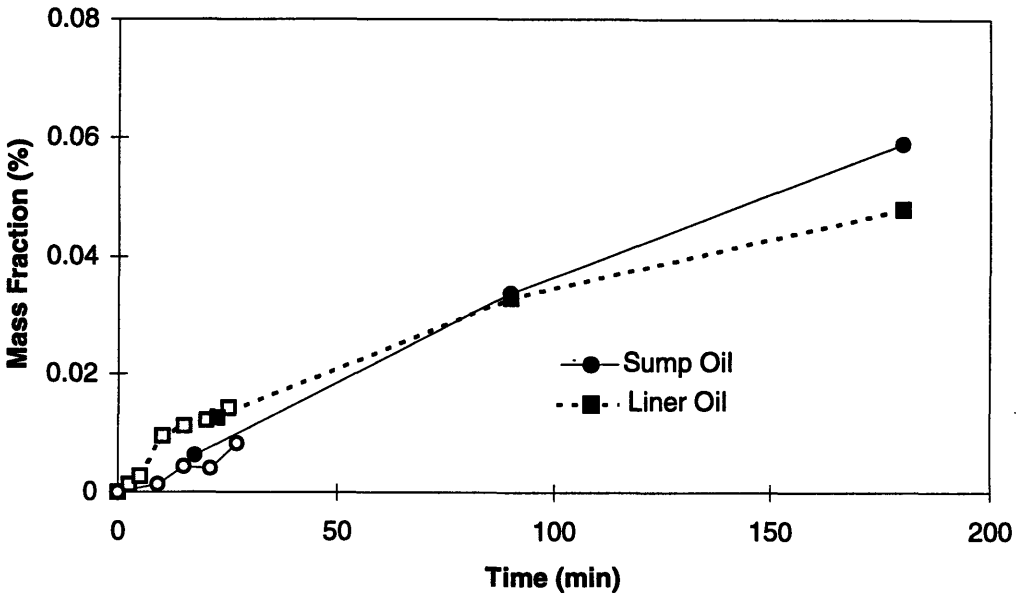

Fig. 3.13 2-methylnaphthalne mass fraction in liner and sump oil for the 3 hour oil sampling experiment. Solid symbols are 3 hour test results. Open symbols are test results from the thrust side warm-up experiment plotted for comparison.

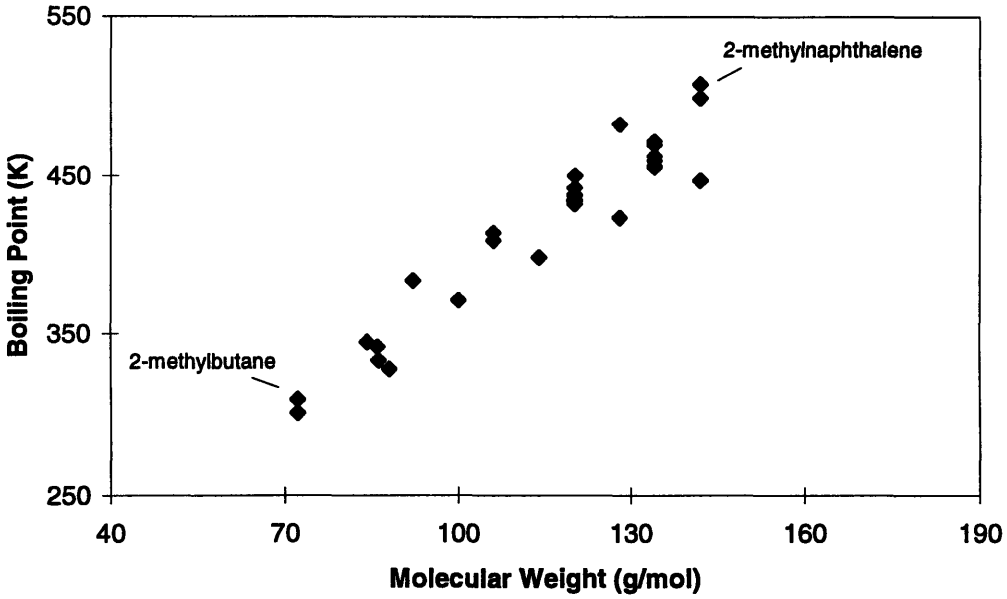

Fig. 3.14 Boiling point vs. molecular weight for some major fuel species in the test gasoline. Points which stack vertically are aromatic compounds in which the benzene ring has the same number of substituents.

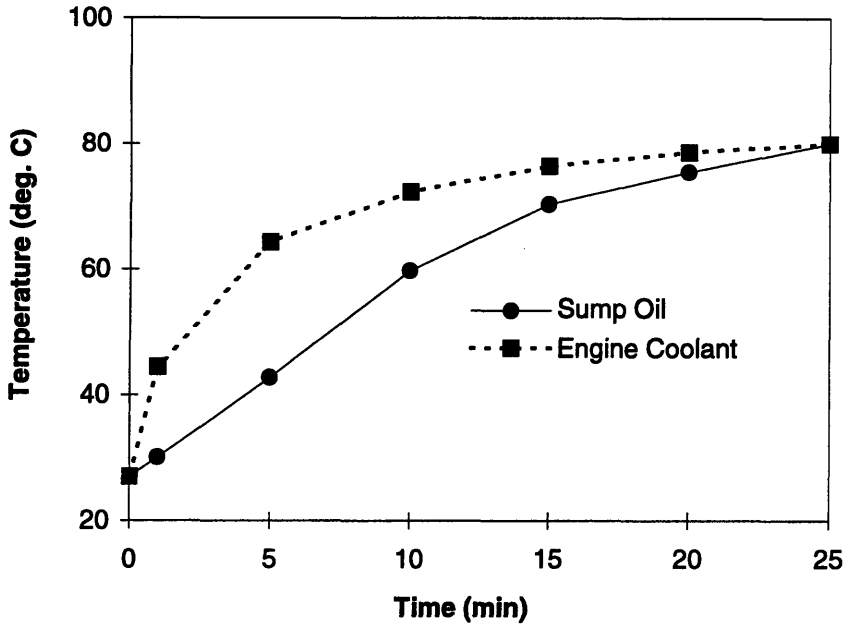

Fig. 3.15 Measured engine coolant and sump oil temperatures during warm-up experiments.

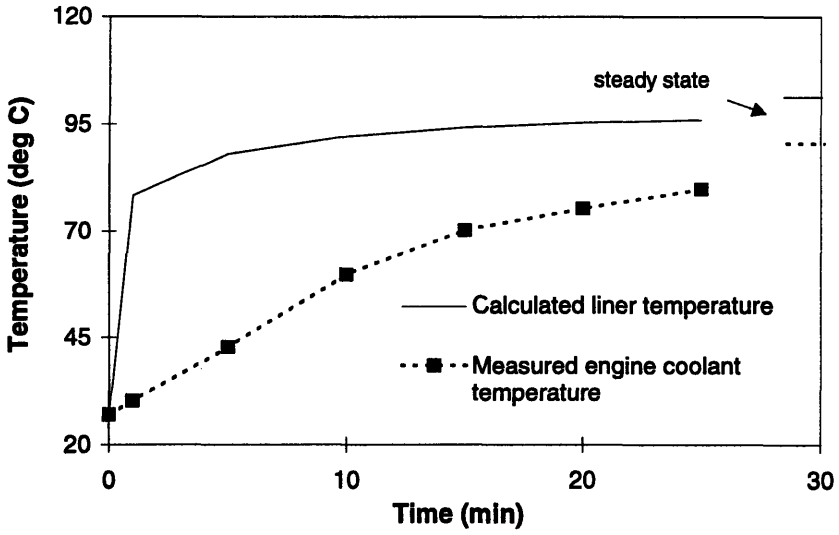

Fig. 3.16 Comparison of calculated cylinder liner temperature with measured engine coolant temperature.

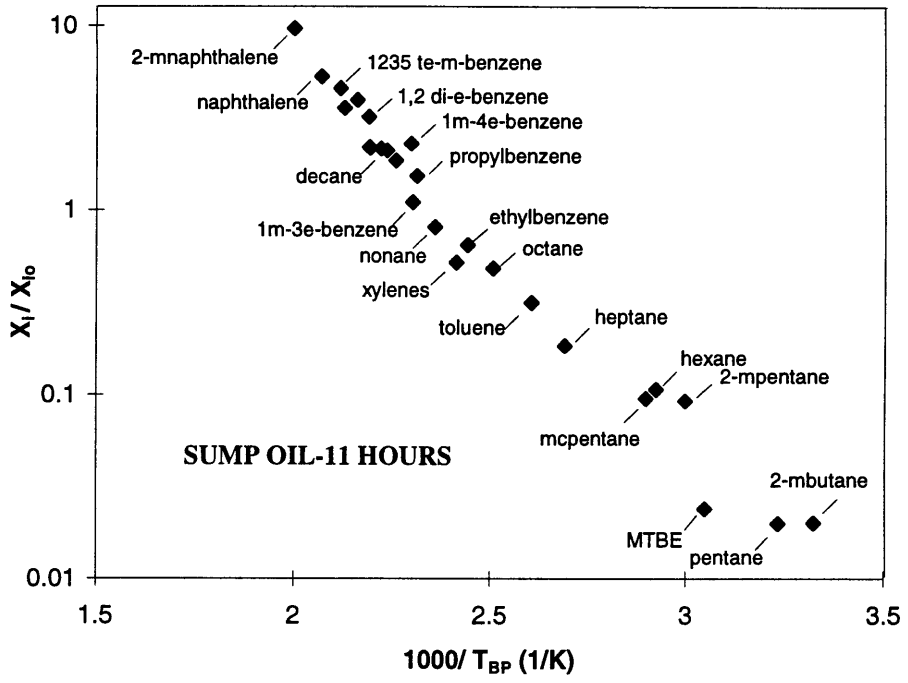

Fig. 3.17 Ratio of the mass fraction of species (relative to total fuel hydrocarbon) in the sump oil relative to the mass fraction of the species in the fuel, after 11 hours of engine operation.

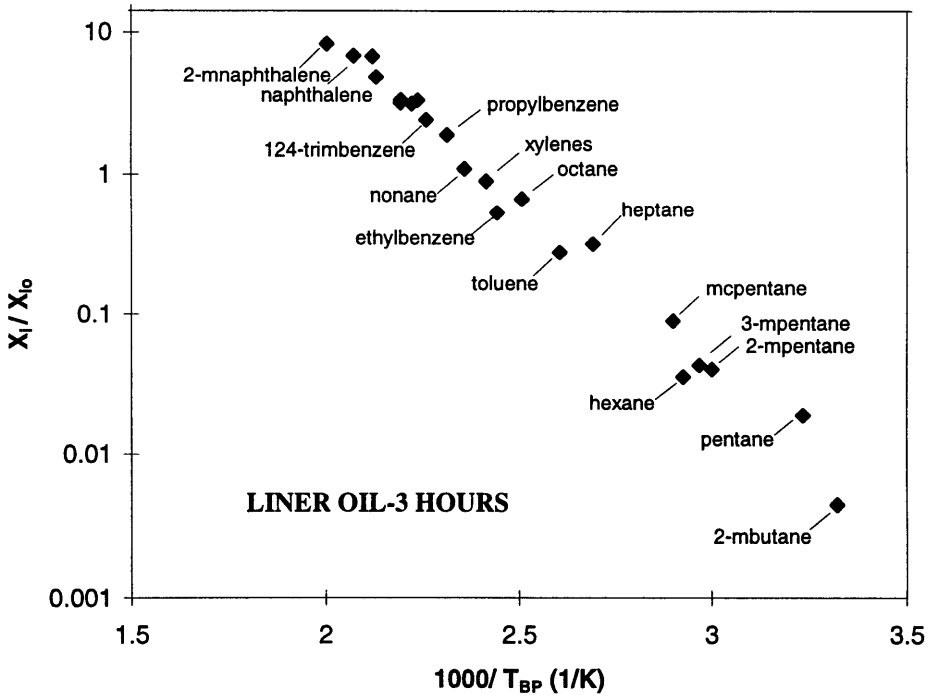

Fig. 3.18 Ratio of the mass fraction of species (relative to total fuel hydrocarbon) in the liner oil relative to the mass fraction of the species in the fuel, after 3 hours of engine operation.

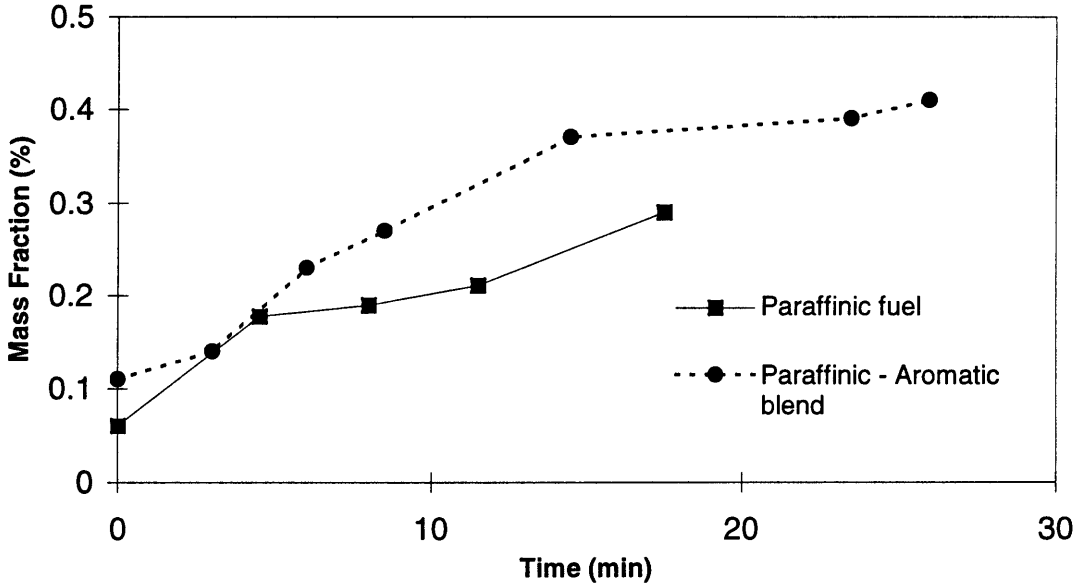

Fig. 3.19 Comparison of total fuel build-up between a paraffinic fuel and one blended with 20% aromatic content.

CHAPTER 4

CRANKCASE GAS SAMPLING EXPERIMENTS

The crankcase gas contains fuel species from a number of sources. The processes which might contribute fuel to the crankcase are desorption of fuel into the crankcase from the liner oil layers, blow-by of the cylinder fuel mixture into the crankcase, and diffusion of fuel components from the sump oil. Furthermore, if the blow-by gas flux to the crankcase is known, the fuel concentration changes in the crankcase gas can be used to estimate the flux of fuel between the liner oil layers and the crankcase gas. Therefore, crankcase gases were sampled and analyzed to determine the distribution of fuel components from warm-up through forty five minutes of engine operation.

4.1 Procedure

A 125 ml (ACE glass, Inc.) glass vessel was prepared for sampling prior to each test. The vessel was cleaned using a sonic cleaner prior to each sampling run to remove residual vacuum grease from the interior. This grease produced a background signal detected by the gas chromatograph FID from fuel absorbed in previous sampling. The sampling vessel was flushed with nitrogen and GC analysis was performed on the nitrogen to ensure that no fuel species were present. The vessel was then evacuated using a vacuum pump and covered in foil to avoid photolytic interaction with the sample.

The crankcase gases were sampled by pumping crankcase gases from the oil dipstick channel into the prepared sampling vessel. The channel was connected to the sampling vessel using Teflon tubing, an adapter, ferrules and a valve. When a sample of crankcase gas was needed, the vacuum pump was activated and the outlet stopcock on the glass vessel was opened. An attached vacuum pressure gauge measured the increase in pressure when the inlet stopcock was opened. After 10 seconds, the inlet and outlet stopcocks were closed and the sample was diluted with nitrogen to reach an acceptable pressure for GC analysis. Only one crankcase gas sample is obtained for each test run, because the sampling might perturb the positive crankcase ventilation flow to the intake manifold and result in erroneous data. The objective of testing was to capture the crankcase gas composition at the selected sampling time. A more accurate sampling method would use heated lines connected to the sampling vessel and a more direct sampling location. Both of these measures would ensure minimal sample condensation. Since the sampling location was adjacent to the exhaust manifold, it was assumed that the temperatures would be sufficiently high to avoid sample condensation.

4.2 Sample Analysis

Gas samples were analyzed with the same gas chromatograph, detector and column choice described in Chapter 3. The Auto/Oil Air Quality Improvement Research Program II method was used for separating the fuel species [17]. Gas flow rates for the detector and analysis method information are included in Appendix B. Quantitative results were obtained using a six component calibration gas which allowed calculation of response factors for fuel components with 1-4 carbon atoms. The response factor is the ratio of the mole fraction of a calibration gas component to the area underneath its peak on an integrated chromatogram. Sample concentration is determined by multiplying the area corresponding to a particular fuel peak by its response factor. For fuel components with more than 4 carbon atoms, the response factor of methane was used, based on experiments and analysis from Kayes [18].

4.3 Results

Crankcase gas samples were obtained in nine sampling runs at the part-load, low speed operating condition used in the oil sampling experiments. The Chevron reformulated gasoline and SH grade engine oil described in Chapter 2 were used in all crankcase sampling runs. Figure 4.1 shows the measured concentration of total HC in the crankcase gas versus time. The total concentration of HC in the crankcase gas increased from 0 to 40,000 ppmC1 after ten minutes of operation, and then stayed nearly constant for the 60 minute duration of the test. Hydrocarbons heavier than xylene were not detected in the crankcase gases. This measurement result was unexpected, since the crankcase HC are expected to be composed mostly of charge. It is possible that condensation of the heavier fuel components was occurring on the oil dipstick tube, within the sampling system, or in the crankcase. Heavy fuel hydrocarbons present in the blow-by which enters the crankcase are easily condensed onto the oil mist in the crankcase and therefore difficult to measure accurately. Light fuel compounds can also be lost by condensation, but it is very possible that the concentrations of the fuel species lighter than xylene were accurately measured. Even though loss of sample was suspected, the concentration of total HC measured in the crankcase gas was very close to the concentration measured by Murakami *et al.* for similar engine speed and load [10]. Murakami *et al.* obtained concentrations using a nondispersive infrared analyzer and were able to identify fuel compounds with more than seven carbon atoms. It was not indicated what fraction of the concentration measured in that study was made up of fuel species greater than seven carbons.

A Rosemount hydrocarbon analyzer with a heated sampling line was also used to measure the total hydrocarbon concentration in the crankcase. At the same sampling location, the concentration of total hydrocarbons measured with the hydrocarbon analyzer was approximately 20,000 ppmC1 lower than the integrated GC measurements described above. The low measured concentration was probably a result of

difficulties in drawing a sample from the partial vacuum in the crankcase (33 kPa) and the suspected condensation problems encountered with the integrated GC measurements.

The detected HC in the crankcase gas are composed primarily of fuel species. After 60 minutes, most fuel species are present at about 1.25% of their concentration in the charge (Fig. 4.2). Non-fuel HC such as ethylene and methane were detected in trace quantities. This data shows that blow-by composition is probably mostly charge, since the presence of non-fuel HC would indicate that blow-by takes place when fuel species have begun to react. Figure 4.2 shows that toluene and heptane are present in lower concentration than species with similar concentrations in the fuel. Heptane and toluene have a high solubility in oil, and may be getting preferentially absorbed in the sump oil.

4.4 Conclusions

A total fuel composition of approximately 40,000 ppm C1 was measured in samples of the crankcase gas. Condensation and absorption of these fuel components prior to obtaining the sample may have occurred. Detected fuel concentrations scaled with the mole fraction of individual species in the total fuel, and the absence of non-fuel HC implies that the blow-by entering the crankcase is composed mostly of charge. The crankcase gas concentration histories obtained from the experimental sampling can be used as inputs to the fuel transport model developed in Chapter 5.

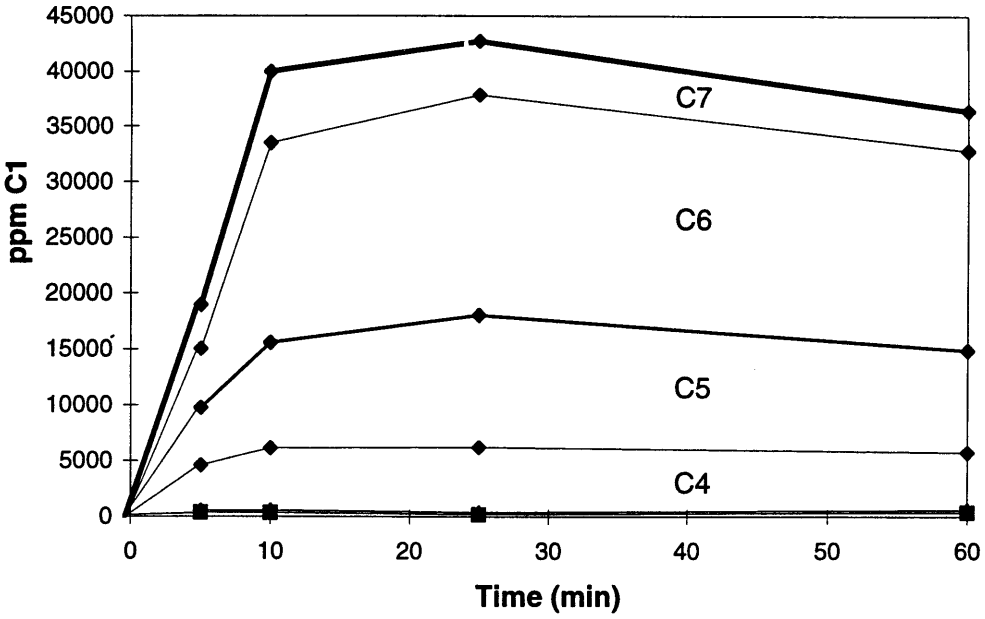

Fig. 4.1 Concentration of crankcase gas HC. The total concentration is denoted by the thick line, and separated into contributions from species with the carbon numbers listed. Regions C1-C3 are present in a total of less than 1000 ppm C1.

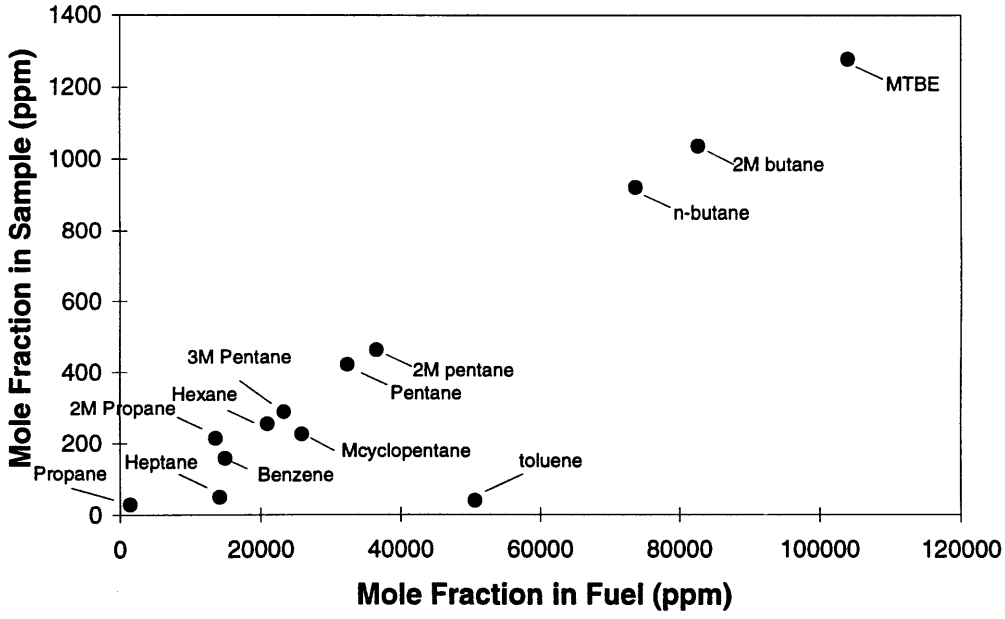

Fig. 4.2 Composition of crankcase gas at 60 minutes. Sample concentration is measured from the crankcase gas and concentration in fuel is the mole fraction of individual species in the fuel.

CHAPTER 5

FUEL TRANSPORT MODEL

One of the objectives of this research was to develop a more complete understanding of the mechanisms for fuel transport within cylinder liner oil layers and throughout the engine. Determining how much fuel is involved in these processes, differences in transport between fuel species, and how the mass fluxes of fuel species change during warm-up and steady state is best determined through a simple mixing model.

5.1 Concept

Fig. 5.1 shows a framework for fuel transport in the oil and crankcase circuits of an internal combustion engine. The shaded rectangles correspond to control volumes from which fuel species enter and exit. These control volumes are connected by lines which represent fuel transport from one control volume to another. Solid lines indicate transport of absorbed fuel species by oil, and dashed lines represent fuel species mass fluxes in the vapor phase. Mass fractions of fuel species in the control volumes are denoted by X_i and mass fluxes of fuel species are represented by $\dot{m}_i$. During engine operation, fuel is inducted along with air into each cylinder of the engine. Following the paths in Fig. 5.1, fuel enters the liner oil control volume as liquid fuel impinging on the liner, or through the fuel absorption process involving cylinder gases. Sinks of fuel present in liner oil are mechanisms by which fuel leaves the oil. These mechanisms include desorption of fuel into the cylinder and crankcase gases. The liner oil can also exchange fuel with blow-by gases, which are in close proximity to ring pack oil. The liner oil is scraped down from the cylinder each cycle, with a fraction of this oil (and the fuel absorbed therein) carried into the sump oil (Fig. 5.1). Sump oil is pumped along the main crankshaft bearings and then splashed back onto the liner. This lubrication process of liner and sump oil exchange is one route by which fuel species travel between the liner oil and sump oil. Fuel can be transported by diffusion between the sump oil and the crankcase gases. Fig. 5.1 shows blow-by gases carrying fuel components into the crankcase gas for a residence period, after which they exit through the positive crankcase ventilation (PCV) valve back into the intake system.

5.2 Fuel Transport Model

The focus of the fuel transport model is determining the direction and magnitude of the mass of fuel species transported between the control volumes of interest: the crankcase gas, the liner oil, and the sump oil. Individual fuel species mass fluxes and the integrated mass flux of all the fuel species are examined in the model. In Fig. 5.1, $\dot{m}_{SC_i}$ is the mass flux of species i transported between the sump and crankcase. The species mass flux between the liner oil layers and crankcase gas is denoted $\dot{m}_{LC_i}$. The

mass fluxes $\dot{m}_{SC_i}$ and $\dot{m}_{LC_i}$ can be calculated by applying mass conservation to the species in the sump oil and liner oil. An estimate of the effect of blow-by gas contribution to fuel species transport can also be made using $\dot{m}_{SC_i}$ and $\dot{m}_{LC_i}$. Also in Fig. 5.1 is $\dot{m}_{\mathrm{PCV}_i}$, which is the species mass flux from the crankcase gas to the positive crankcase ventilation valve.

Blow-by gases containing fuel species interact with liner oil films before entering the crankcase. This study does not include measurements of blow-by gas fuel concentrations near the ring pack. Instead, the mass fraction of fuel in blow-by is derived from crankcase gas measurements of CO_2 described in section 5.3. Therefore, the mass flux of fuel species in blow-by $\dot{m}_{BC_i}$, is modeled as entering the crankcase without interacting with liner oil layers. Blow-by fuel exchange with the liner oil is lumped with the mass flux of fuel species transported between the crankcase gas and the liner oil layer, $\dot{m}_{LC_i}$. The diagram in Fig. 5.2 reflects these simplifications, and will be used to represent transport processes in the engine oil. This figure is useful in understanding the discussion of the fuel transport model that follows in the remainder of this chapter.

5.3 Model Inputs

This section describes various inputs to the fuel transport model that were needed in order to realistically describe the transport of fuel within the oil and crankcase gases. The areas examined are: the liner oil layers, oil refreshment rate and oil film thickness.

5.3.1 Liner Oil Layers

The method used to estimate the total volume of oil in the cylinder for this study is based on oil film thickness (OFT) measurements made by lubrication researchers. The oil film was measured in a Kohler spark-ignited engine operating at a similar speed and load as the engine in this study, with similar piston and bore geometry [19]. The Kohler engine used 10W-30 mineral oil, while the engine in this work operated with 5W-30 mineral oil. Nevertheless, Kohler engine data was used to make estimates of oil film thickness for the calculations in the fuel transport model. An estimate of the range of OFT on the free liner and piston skirt is shown for the time periods when the piston is at bottom center, mid-stroke, and top center (Fig. 5.3). In reality, the OFT can change during engine warm-up, and values may vary depending on whether the piston is in downstroke or upstroke [20]. The OFT ranges are intended to be wide enough to account for these and other uncertainties (bore distortion, honing volume, etc.). A simple equation for the volume of liner oil, V_i, in region i is:

$$V_i = \pi B \delta_i l \tag{5.1}$$

for a cylinder with bore B, region with oil film thickness δ, and liner length l. The land and piston geometry were measured using precision calipers, so that the oil volume there could be accurately calculated. An expression for the volume of oil on a region of the piston skirt or land with length l is

$$V_l = 2\pi(\frac{D}{2})\delta l \tag{5.2}$$

where D is the diameter of the piston.

The volume of oil in the ring pack is approximated as constant for all time and piston positions. The estimated volume of oil on the lands and in the ring grooves, along with dimensions used in OFT calculations are shown in Fig. 5.4. The amount of oil in the ring grooves is calculated by estimating what fraction of each groove is flooded, excluding the piston ring volume. The volume of oil in a particular ring groove can be estimated as

$$V_i = 2\pi\varphi hd(\frac{D}{2} - d) \tag{5.3}$$

for a piston of diameter D, groove height h, groove depth d, and flooded fraction φ. Using these estimates, the total volume of oil in one cylinder was calculated to be approximately 2 cm^3. The largest contribution to the total volume of oil is from the flooded oil control ring groove and the lower liner, which together make up almost 1.6 cm^3.

Calculating the volume of oil on the liner is necessary in order to evaluate the mass of fuel species from measured concentration data. If an accurate value for the volume (and subsequently the mass) of the oil is known, the mass of the fuel species on the liner at a given time can be evaluated from GC measurements of the mass fraction of fuel species in oil. The oil film on the liner was modeled as a well-stirred volume of oil consisting of the regions described above. The assumption of thorough mixing along the length of the liner is assumed to be valid for the time scale at which oil was sampled [20]. Therefore, fuel concentrations in oil sampled from the piston skirt region may be considered representative of values throughout the liner oil layer. It is assumed that fuel concentrations are not varying circumferentially around the liner, nor from cylinder to cylinder. These simplifications were partly supported by measurements made on opposite sides of the piston (Chapter 3). The oil films which coat the cylinder head were not considered in this study, since their participation in transport processes is likely to be small.

The viscosity of oil on the liner decreases with increasing engine temperature during the warm-up phase. The decrease in oil viscosity reduces the oil film thickness and therefore, the total volume of oil on the liner may be over-predicted [15]. Absorbed fuel has a smaller effect on the decrease of oil viscosity. Both of these phenomena were not modeled since they are of little importance in the regions that contribute the largest volume of oil to the cylinder: the lower liner oil and oil control ring groove.

5.3.2 Oil Refreshment Rate

An important input to the fuel transport model is the mass flow rate of oil between the sump and the liner oil layers, $\dot{m}_{oil}$ (Fig. 5.5). This oil exchange rate can be expressed as the percentage of the mass of cylinder liner oil that is replaced each revolution, which is termed the refreshment rate, R. This calculation requires a value for the mass of liner oil (Section 5.3.1). The refreshment rate is calculated by using sump and liner oil HC species measurements of absorbed heavy fuel species during the first 10 minutes of engine operation. At this time, the engine coolant and oil are relatively cool, so high molecular weight fuel species are unlikely to be transported in the gas phase ($\dot{m}_{SC_i}$, $\dot{m}_{LC_i}$ = 0). During this period, it was assumed that the only flux of heavy fuel species into and out of the sump oil is by absorbed fuel in the flow of oil between the sump and liner (Fig. 5.5). Applying mass conservation to species i in the sump oil results in

$$4\dot{m}_{oil}(X_{Li} - X_{Si}) = M_S \frac{dX_{S_i}}{dt} \tag{5.4}$$

where $\dot{m}_{oil}$ is the mass flow rate of oil between the liner and sump for one cylinder, X_{L_i} and X_{S_i} are the mass fractions of fuel species i in the oil, and M_S is the mass of sump oil. The mass fractions X_{L_i} and X_{S_i} are obtained from the measurements of 1,2,4-trimethylbenzene and naphthalene discussed in Chapter 3 and shown in Figs. 3.4 and 3.5. A factor of four is included in Eq. 5.4 since the oil from four cylinders is being exchanged with sump oil. The refreshment rate R is defined as

$$R = \frac{\dot{m}_{oil}}{M_L \cdot N} \tag{5.5}$$

where N is engine speed. The calculated refreshment rate (Fig. 5.6) is between 1% and 3%, depending on the fuel species mass fractions used as input to Eqs. 54 and 5.5. Using naphthalene fuel concentrations as an input results in a constant refreshment value of 1.25%. The refreshment rate calculated using 1,2,4-trimethylbenzene measurements is not constant, probably due to gas transport with the crankcase gases. The calculated refreshment rate agrees well with Norris' estimate of refreshment rate, which adds confidence to the estimate of liner oil volume discussed in Section 5.3.1 [8].

5.3.3 Blow-by Gas

In order to model fuel transport to or from the crankcase gas, the rate at which blow-by gas enters and exits the crankcase is needed. The engine used in this study had no fresh air dilution to the crankcase gases, since the fresh air hose was sealed (Fig 5.7). Therefore, when the crankcase is sufficiently filled with gas, the flow rate leaving the PCV valve is equal to the flow rate of blow-by. A simple experiment was conducted to measure the volume flow rate of crankcase gas exiting through the PCV hose. A tube attached

to the end of the PCV hose was immersed in a tank of water (Fig. 5.8). The volume of water displaced when the engine is operating is then equal to the blow-by flow rate into the crankcase. The measured flow-rate of blow-by into the crankcase at start-up was 12 L/min, which corresponds to 2.6% of the charge. Blow-by was reduced to 6 L/min after 5 minutes, which may be the result of better sealing between the piston rings and liner as the engine warmed. These values compare favorably with measurements made by previous researchers on similar engines [4]. The mass flow rate of blow-by is calculated by multiplying the measured volume flow rate by the density of air at the measured crankcase temperature of 60 °C and pressure of 33 kPa (absolute).

The mass flux of fuel species in the blow-by gas is $\dot{m}_{BC}$ (Fig. 5.2). The concentration of CO_2 was measured in the crankcase gas to determine $\dot{m}_{BC}$. The crankcase CO_2 concentrations rise to a steady state concentration of 2.25% after five minutes. This is the time required to fill the crankcase with combustion gas CO_2, which diffuses out of the crankcase after the engine is stopped. As described above, the crankcase is a closed circuit with no fresh air dilution. Therefore, the only source of CO_2 to the crankcase is from blow-by. Comparing the concentration of CO_2 in the crankcase gas with the amount present in the cylinder, an estimate of the fraction of charge in blow-by can be made.

The mass fraction of residual gas in typical four valve engines operating at the engine conditions of this study is approximately 15% [4]. It was assumed that the residual gas in the cylinder contains the same concentration of CO_2 as exhaust gas. The cylinder always contains the CO_2 present in the residual gas. The mass fraction of CO_2 present in unburned charge is negligible ($3 \cdot 10^{-4}$). Depending on the crank angle there will also be CO_2 in the cylinder present from the cylinder burned gas. The cylinder concentration of CO_2 at a specific point in a cycle can thus be expressed as:

$$X_{CO_2}^{cyl} = f_r(X_{CO_2}^{b}) + (1-(f_{ch}+f_r))X_{CO_2}^{b} \tag{5.6}$$

where f_r is the cylinder residual mass fraction, $X_{CO_2}^{b}$ is the mass fraction of CO_2 in burned cylinder gases, and f_{ch} is the mass fraction of unburned charge in the cylinder. In a simplification of the blow-by process, we assume that the measured crankcase concentration of CO_2 is equal to $X_{CO_2}^{cyl}$ when blow-by occurs. The only unknown in Eq. 5.6 is f_{ch}, the fraction of unburned charge in the cylinder when blow-by occurs, which therefore, is the fraction of charge in blow-by. Solving Eq. 5.6 for f_{ch} yields 86% for the fraction of charge in blow-by. This result is consistent with the distribution of fuel components observed in the crankcase sampling of Chapter 4.

Table 5.1: Values for the estimate of fuel fraction in blow-by gas

burned gas residual mass fraction in cylinder (estimated)	0.15
mole Fraction of CO_2 in burned gas (stoichiometry)	0.13
mole fraction of CO_2 in crankcase gas (measured)	0.025
calculated mass fraction of charge in crankcase	0.86

5.4 Sump Oil Control Volume

The method used to determine the species mass fluxes between different control volumes is to apply mass conservation to fuel species in the three control volumes using measured species data and the model inputs described in Section 5.3. The control volume containing the smallest number of species fluxes entering and leaving is the sump oil (Fig 5.5). Absorbed fuel species enter the sump with the scraped-down liner oil, which has a fuel species mass fraction X_{L_i}. The mass flux of fuel species entering the sump oil from the liner oil is expressed as $4\dot{m}_{\text{oil}} X_{L_i}$, where $\dot{m}_{\text{oil}}$ is the mass flow rate of oil scraped down from one cylinder and the factor 4 is included to account for oil flow from the 4 cylinders down into the sump. Similarly, sump oil is splashed onto the liner, carrying away absorbed fuel from the sump. Therefore, the mass flux of fuel species leaving the sump oil is $4\dot{m}_{\text{oil}} X_{S_i}$. The only other species flux interacting with the sump oil is the flux of species diffusing between the crankcase gas and the sump oil, $\dot{m}_{SC_i}$. It is possible to obtain an expression involving $\dot{m}_{SC_i}$ by applying mass conservation to the species i in the sump control volume as follows:

$$M_S \frac{dX_{S_i}}{dt} = 4\dot{m}_{\text{oil}}(X_{L_i} - X_{S_i}) + \dot{m}_{SC_i} \tag{5.7}$$

where M_S is the mass of sump oil. The direction and magnitude of $\dot{m}_{SC_i}$ is obtained in this manner using the measured species mass fractions X_{S_i} and X_{L_i}.

5.5 Results from the Sump Oil Control Volume

Several fuel components in the gasoline were chosen as model inputs to highlight any transport differences resulting from molecular weight, structure or solubility. The fuel components selected from the GC analysis data are listed in Table 5.2. 2-methylpentane is one of the lightest fuel components in the gasoline used, and 2-methylnaphthalene is one of the heaviest. The single ring aromatics chosen are distributed evenly among the range of molecular weights appearing in the test fuel. The fuel chromatogram in Fig. B1 (Appendix B) shows the distribution of fuel components in the test fuel. The fuel composition is skewed, since 87% of the alkanes in the fuel contain seven carbons or less, while the heavy components are

mostly aromatic species. 'Total fuel HC' in Table 5.2 is the mass fraction of all fuel species in each oil sample, obtained by integrating the areas of all fuel species in a sample chromatogram. Using this integrated data as an input to the calculations in this section gives averaged mass fluxes for all the fuel species in the oil. The fuel species in Table 5.2 were also chosen because they were present in sufficient quantities in the oil to make accurate measurements.

Table 5.2 Fuel components chosen as modeling inputs

Fuel Component	Chemical Group	Molecular Weight (g/mol)
2-methylpentane	Alkane	86.18
toluene	Aromatic	92.14
xylenes	Aromatic	106.17
1,2,4-trimethylbenzene	Aromatic	120.20
2-methylnaphthalene	Aromatic (PAH)	142.20
total fuel HC	Alkanes, Aromatics, Olefins, Ethers	-

The results obtained in the sump control volume are the magnitude and direction of $\dot{m}_{SC_i}$, the mass flux of species *i* between the crankcase gas and the sump oil. The species mass flux $\dot{m}_{SC_i}$ is determined by solving Eq. 5.7. The input mass fractions X_{S_i} and X_{L_i} are obtained from the oil sampling experiments described in Chapter 3 (Figs. 3.10-3.13). A polynomial curve fit is used for the species mass fractions in each of the data plots resulting in the curve-fit data used as an input to Eq. 5.7 (Fig. 5.9). The curve fits smooth the data to allow for the differentiation in Eq. 5.7. In this manner, $\dot{m}_{SC_i}$ was computed for the fuel species of interest. The magnitude of the species mass flux $\dot{m}_{SC_i}$ was then normalized by the rate that each of the species is injected into the cylinder during stoichiometric engine operation, $\dot{m}_{\mathrm{inj}_i}$. The corresponding fraction, $\dot{m}_{SC_i} / \dot{m}_{\mathrm{inj}_i}$ is shown in Fig 5.10.

An average transport rate and direction for all fuel species is given by inputting the total fuel HC mass fractions X_S and X_L into Eq. 5.7. Recall that the total fuel HC is the sum of all the fuel species in the gasoline. For the total fuel HC (Fig. 5.10), $\dot{m}_{SC}$ is always directed from the crankcase gas to the sump and $\dot{m}_{SC}/\dot{m}_{\mathrm{inj}}$ increases from 0.3% at 10 minutes, to 1.6% after 3 hours. During warm-up, this ratio is low except for a sharp peak during the first 5-10 minutes. In Eq. 5.7, this peak results from the liner fuel concentration increasing at a rate which is not high enough to account for the increase in sump oil. The validity of the first sampling points (at 2.5 minutes and 5 minutes) may influence calculations during this time period. Another small peak in $\dot{m}_{SC}/\dot{m}_{\mathrm{inj}}$ is shown in Fig. 5.10 at approximately 25 minutes, and can also be seen in the liner species mass fractions in Fig. 5.9.

The evolution of $\dot{m}_{SC}$ for the total fuel HC is similar to that of the individual fuel species (Fig. 5.10). The fuel species shown are ordered by increasing molecular weight from right to left, and from bottom to top. For the fuel components shown, the magnitude of $\dot{m}_{SC\,i} / \dot{m}_{\mathrm{inj}_i}$ after warm up generally increases with molecular weight. The species mass flux $\dot{m}_{SC_i}$ is directed from the crankcase gas to the sump oil for all of the species for most of the three hour engine running time. In Fig. 5.10, 1,2,4-trimethylbenzene is the only species with $\dot{m}_{SC_i}$ directed from the sump oil to the crankcase gas between 100 and 150 minutes of engine operation.

The magnitude of $\dot{m}_{SC\,i} / \dot{m}_{\mathrm{inj}_i}$ is substantially higher for 2-methylnaphthalene compared to the total fuel HC and the other fuel species. At three hours of engine operation, 2-methylnaphthalene is transported to the sump oil from the crankcase gas at 13% of the rate that 2-methylnaphthalene is injected into the cylinders (Fig. 5.10). This can partly be extracted from 2-methylnaphthalene data in Fig. 5.9, where the sump oil mass fraction of 2-methylnaphthalene is larger than the liner oil mass fraction. Additionally, the slope of the mass fraction of 2-methylnaphthalene (dX_{S_i}/dt) in the sump oil is high. Both of these factors increase the magnitude of $\dot{m}_{SC_i}$ in Eq. 5.7. Finally, since 2-methylnaphthalene is less than 1% of the injected fuel, the ratio $\dot{m}_{SC_i} / \dot{m}_{\mathrm{inj}_i}$ is also high. It is unlikely that the inputs X_{S_i} and X_{L_i} in Eq. 5.7 are in error, since 2-methylnaphthalene mass fractions in oil do not deviate from other absorbed fuels of similar molecular weight, as seen in Chapter 3 (Fig. 3.19). This large magnitude of $\dot{m}_{SC_i}$ does not appear to be a characteristic of polynuclear aromatic hydrocarbon transport, either. The same normalized fluxes calculated for naphthalene are approximately 3% of the injected amount at three hours. The high boiling points of the heavy fuel species may be responsible for their higher percentage in the engine oil.

The time necessary for the species mass flux $\dot{m}_{SC_i}$ to reach a steady state is the same as that required for the fuel concentrations in the oil to reach steady state. Therefore, $\dot{m}_{SC_i}$ approaches steady state within three hours for 2-methylpentane, toluene and xylene, while $\dot{m}_{SC_i}$ is still increasing for the other fuel species. Since heavy fuel species make up a large percentage of the fuel in the oil, the plots of $\dot{m}_{SC\,i} / \dot{m}_{\mathrm{inj}_i}$ in Fig. 5.10 for the heavier fuel components bear a strong resemblance to the same plot for the total fuel HC. Except for the high magnitude of 2-methylnaphthalene transport, the species mass flux from crankcase gas to the sump oil appears to be a fairly consistent process across all the fuel species examined.

5.6 Liner Oil Control Volume

The fluxes of fuel species interacting with the liner oil control volume are more complicated than those encountered with the sump oil control volume (Fig. 5.12). Again, oil is splashed up from the sump generating a species mass flux of absorbed fuel components to one cylinder liner. This flux can be expressed as $\dot{m}_{\mathrm{oil}} X_{S_i}$. As discussed for the sump oil control volume, the liner oil is scraped down from the

cylinder, which represents a fuel species mass flux out of the liner. This flux term is $\dot{m}_{\text{oil}} X_{L_i}$. The liner oil control volume consists of only the oil in one of the four engine cylinders, so the mass fluxes are not multiplied by 4 as in the sump oil control volume. Fuel species in the liner oil layer are absorbed and desorbed between the cylinder gas, the crankcase gas and blow-by. As shown in Fig. 5.12, $\dot{m}_{LC_i}$ is the species mass flux between the crankcase gases and the liner oil. Also lumped in $\dot{m}_{LC_i}$ is the flux between the blow-by gas and the liner oil. The remaining flux term in Fig. 5.12 is $\dot{m}_{\text{abs}_i}$. The mass species flux $\dot{m}_{\text{abs}_i}$ groups the species mass fluxes from absorption and desorption of cylinder gases (not including blow-by), as well as the species mass fluxes from oil consumption and liquid fuel impingement. It is possible for $\dot{m}_{\text{abs}_i}$ to be positive or negative depending on the magnitude of the individual species mass fluxes. The terms appearing in the conservation of the mass of fuel species *i* in the liner oil are

$$M_L \frac{dX_{L_i}}{dt} = \dot{m}_{\text{oil}}(X_{S_i} - X_{C_i}) + \dot{m}_{LC_i} + \dot{m}_{\text{abs}_i} \tag{5.8}$$

where M_L is the mass of oil on the liner. The unknown terms in Eq. 5.12 are $\dot{m}_{LC_i}$ and $\dot{m}_{\text{abs}_i}$. Again grouping the unknown fluxes together, Eq. 5.8 becomes

$$M_L \frac{dX_{L_i}}{dt} = \dot{m}_{\text{oil}}(X_{S_i} - X_{C_i}) + \dot{m}_{\text{net}_i} \tag{5.9}$$

where $\dot{m}_{\text{net}_i}$ is the net mass flux of species absorbed in the liner oil, excluding the contributions of fuel transport by $\dot{m}_{\text{oil}}$.

5.7 Results from the Liner Oil Control Volume

The flux calculated in this section, $\dot{m}_{\text{net}_i}$, is the net (non-oil transport) fuel species interaction with the liner oil layer. Eq. 5.9 is used to calculate $\dot{m}_{\text{net}_i}$, and the inputs to Eq. 5.9, X_{S_i} and X_{L_i} are again from the curve-fit experimental data in Fig. 5.9. The magnitude of $\dot{m}_{\text{net}_i}$ for each of the species in Table 5.2 is again normalized by the rate that each of the species is injected into the cylinder during stoichiometric engine operation, $\dot{m}_{\text{inj}_i}$. The ratio ($\dot{m}_{\text{net}_i} / \dot{m}_{\text{inj}_i}$) is plotted in Fig. 5.11.

The integrated fuel species value of $\dot{m}_{\text{net}}$ is examined first. The total fuel HC plot in Fig. 5.11 shows that the mass flux $\dot{m}_{\text{net}}$ is towards the liner oil layer during the first 70 minutes of engine operation. For this time period, there is a net flux of total fuel HC <u>from</u> blow-by, crankcase gas, cylinder gas and liquid fuel impingement <u>to</u> the liner oil. After this point, the direction of the net mass flux changes, and $\dot{m}_{\text{net}}$ is negative, based on the sign convention used in Eq. 5.9. This corresponds to a mass flux of total fuel HC from the liner oil which is apportioned to the cylinder gas, crankcase gas, or blow-by. The ratio

$\dot{m}_{net} / \dot{m}_{inj}$ is less than 2% for the three hour engine test duration. This ratio is about 1.8% after ten minutes and decreases steadily until it reaches -1.8% after three hours of engine operation.

The species mass fluxes $\dot{m}_{net_i}$ share similar characteristics to $\dot{m}_{net}$ for the total fuel HC. The species mass fluxes $\dot{m}_{net_i}$ are initially positive, at which time the $\dot{m}_{net_i}$ becomes negative (and the liner oil becomes a source of fuel species) varies depending on the molecular weight of the fuel species. For instance, in Fig. 5.11, $\dot{m}_{net_i}$ is negative for 2-methylpentane after 10 minutes of engine operation, while it remains positive for 1,2,4-trimethylbenzene until nearly 180 minutes. The sign change in $\dot{m}_{net_i}$ occurs approximately when X_{S_i} is equal to X_{L_i} in Eq. 5.9, which is also visible in Fig. 5.9. The magnitude for 2-methylnaphthalene transport is again higher than for other species, with $\dot{m}_{net_i} / \dot{m}_{inj_i}$ changing from 8% to -8% over the duration of the test (Fig. 5.11). The species mass flux $\dot{m}_{net_i}$ is nearly zero for 2-methylpentane for the three hours of engine operation. This indicates that the transport mechanisms grouped in $\dot{m}_{net_i}$ do not involve the light paraffins, or that the processes in $\dot{m}_{net_i}$ are offsetting each other.

5.8 Crankcase Gas Control Volume

The model of fuel transport between the crankcase gas and the engine oil is structured in a similar manner to the model of fuel species interaction with the liner and sump oil. A crankcase gas control volume is defined with mass fluxes of fuel species interacting with the control volume. Through mass conservation of the species in the crankcase control volume, additional information about the species mass fluxes interacting with the engine oil is obtained (Fig. 5.13). The species mass flux of fuel between the crankcase gas and the sump oil, $\dot{m}_{SC_i}$ was already calculated in section 5.6 using Eq. 5.7 and oil sampling data. There are three other fluxes interacting with the crankcase gas: $\dot{m}_{PCV_i}$, $\dot{m}_{LC_i}$ and $\dot{m}_{BC_i}$. The species mass flux $\dot{m}_{LC_i}$ is the transport of fuel species between the liner oil layer and both the crankcase gas and blow-by. The term $\dot{m}_{BC_i}$ is the species mass flux entering the crankcase gas from blow-by. The species which exit the crankcase via the PCV valve are represented by $\dot{m}_{PCV_i}$. Both $\dot{m}_{PCV_i}$ and $\dot{m}_{BC_i}$ were determined experimentally. Under steady state conditions, the species mass flux $\dot{m}_{BC_i}$ through the PCV valve can be expressed as

$$\dot{m}_{BC_i} = f_{ch} \dot{m}_{BB} w_i \tag{5.10}$$

where f_{ch} is the mass fraction of charge in blow-by, $\dot{m}_{BB}$ is the mass flow rate of blow-by gas in the crankcase, and w_i is the mass fraction of fuel species i in the charge. Section 5.3.3 described the technique

used to calculate f_{ch} and the volume flow rate of blow-by. The mass fraction w_i is obtained from stoichiometry and GC analysis of the total fuel. The species mass flux $\dot{m}_{\mathrm{PCV}_i}$ is

$$\dot{m}_{\mathrm{PCV}_i} = \dot{m}_{\mathrm{BB}} X_{CC_i} \tag{5.11}$$

where X_{CC_i} is the mass fraction of fuel species i in the crankcase gas. The mass flow rate $\dot{m}_{\mathrm{BB}}$ is constant for both Eqs. 5.10 and 5.11. Applying mass conservation to the species in the crankcase control volume (Fig. 5.13) produces the expression

$$M_{CC} \frac{dX_{CC_i}}{dt} = \dot{m}_{BC_i} - \dot{m}_{SC_i} - \dot{m}_{LC_i} - \dot{m}_{\mathrm{PCV}_i} \tag{5.12}$$

where M_{cc} is the mass of crankcase gases. This expression can be solved for $\dot{m}_{LC_i}$ so the crankcase gas and blow-by gas contribution to liner oil transport can be determined. In section 5.7, $\dot{m}_{net\,i}$ was determined as the sum of $\dot{m}_{LC_i}$ and $\dot{m}_{abs\,i}$. Therefore, solving Eq. 5.12 for $\dot{m}_{LC_i}$ gives the magnitude of $\dot{m}_{abs}$, the flux term described in section 5.6. While $\dot{m}_{SC_i}$ in Eq. 5.12 is dependent on the results of the sump control volume, the other terms are independent of the previous calculations involving the engine oil.

5.9 Results from the Crankcase Gas Control Volume

The term discussed in this section is the species mass flux $\dot{m}_{LC_i}$, calculated by solving Eq. 5.12. The inputs into this equation are the measured species mass fractions in the liner and sump oil, the measured crankcase gas species mass fractions, and the species mass flux $\dot{m}_{BC\,i}$ and $\dot{m}_{\mathrm{PCV}_i}$ described in Section 5.8. A polynomial curve fit was again applied to the crankcase gas concentrations X_{CC_i} and is shown in Fig. 5.14. In Fig. 5.15 the ratio $\dot{m}_{LC_i} / \dot{m}_{\mathrm{inj}_i}$ is plotted for 2-methylpentane and toluene along with the previously calculated $\dot{m}_{net} / \dot{m}_{\mathrm{inj}_i}$. For 2-methylpentane, the direction of $\dot{m}_{LC_i}$ is negative, transport is from the liner oil layer to either the crankcase gas or blow-by. The magnitude of $\dot{m}_{LC_i} / \dot{m}_{\mathrm{inj}_i}$ ranges between -1.4% and 0% during the 60 minutes of engine operation for which input data to Eq. 5.12 is available. Since $\dot{m}_{net\,i}$ is the sum of $\dot{m}_{LC_i}$ and $\dot{m}_{abs\,i}$, Fig. 5.15 shows that for 2-methylpentane the direction of $\dot{m}_{abs\,i}$ must be to the liner in order for $\dot{m}_{net\,i} / \dot{m}_{\mathrm{inj}_i}$ to be nearly zero.

Solving Eq. 5.12 with toluene as the input fuel species, it is determined that the mass flux $\dot{m}_{LC_i}$ is directed to the liner oil layer. This direction is opposite of what was observed with 2-methylpentane. The magnitude of $\dot{m}_{LC_i} / \dot{m}_{\mathrm{inj}_i}$ varies between 0% and 1%, with the irregularity in Fig. 5.15 coming as a result of the changes in $\dot{m}_{SC_i}$ observed in Fig. 5.10. The plots of $\dot{m}_{LC_i} / \dot{m}_{\mathrm{inj}_i}$ and $\dot{m}_{net\,i} / \dot{m}_{\mathrm{inj}_i}$ in Fig. 5.15 are nearly identical for toluene during the first 25 minutes. For this warm-up period, the species mass flux $\dot{m}_{abs\,i}$ is

nearly zero. After this time, the magnitude of $\dot{m}_{LC_i} / \dot{m}_{\mathrm{inj}_i}$ is about 1% higher than $\dot{m}_{net\,i} / \dot{m}_{\mathrm{inj}_i}$, which means that $\dot{m}_{abs}$ is negative, and the liner oil acts a source of fuel species to the cylinder gases.

Complete box diagrams of the light, intermediate, and heavy species fluxes discussed in Sections 5.4-5.9 are shown in Figs. 5.16-5.17. The box diagrams are arranged similar to Fig. 5.2, which gives the species fluxes between the three control volumes of interest. In Fig. 5.16, the species mass fluxes at the end of warm-up (approximately 30 minutes) are shown. The species fluxes immediately to the right of the liner oil are $\dot{m}_{net\,i}$, the total (non-oil) transport to the liner oil. The two species fluxes to the left of the crankcase gas control volume are the species fluxes $\dot{m}_{LC_i}$, the species mass flux between the liner oil layer and both the crankcase gas and blow-by gas. Fig. 5.17 is a similar box diagram for three hours of engine operation. Figure 5.18 is a box diagram comparing the total fuel mass fluxes at warm-up and steady state. Particularly evident in the box diagrams of the individual fuel species (Figs. 5.16-5.17) is the role of liner oil layers as sources of light hydrocarbons to the crankcase gas, and the build-up of heavy hydrocarbons in the sump oil.

5.10 Uncertainty Analysis

In order to model the transport of fuel in the oil and crankcase gases, simplifications, experimental measurements, and assumptions were made which introduce uncertainty into the results. As discussed in section 5.3, there were a number of assumptions made concerning the oil layer thickness and distribution in the cylinder. These assumptions affect the calculated mass of fuel species in the oil, and therefore propagate uncertainty in calculations involving this term. The uncertainty in gas chromatography analysis of experimental data, while minimized by frequent calibration, was also estimated. Errors in the structure of the model, such as neglect of a transport route or attributing a single flux to the result of a number of fluxes, usually lead to inconsistencies in a model. One purpose of the crankcase gas calculations, which were not completely dependent on oil sampling data, was a consistency check with other model calculations. Since the mass fluxes calculated using crankcase gas data are, for instance, not greater than the amount of fuel injected, it is unlikely that a major error in model structure is present.

In Table 5.3, the uncertainties associated with model inputs are listed. These terms are the inputs to Eqs. 5.7, 5.9 and 5.12. The value used for the volume of oil on the cylinder liner was 2 cm^3, based on the analysis of Section 5.3. The liner oil refreshment rate calculated using the estimated liner oil volume also agreed well with other studies. Varying the bounds on oil film thickness from the lowest values seen in the Kohler experiments to the highest values [19,20], it is likely the volume of oil is between 2.25 cm^3 and 1.75 cm^3. It is not unusual, however, for uncertainty in the cylinder oil volume to range as high as ±50%. Using the bounds mentioned above, the fractional uncertainty in the liner oil mass M_L is ±12.5%. Based on sample repeatability and a calibration sample, the fractional uncertainty in GC measurements, and therefore X_L and

X_S, is estimated as ±5%. This uncertainty assumes that errors in GC measurements are random. The uncertainty associated with the crankcase gas measurements of the light HC is more difficult to estimate. If the concentration of identified fuel species was not decreased by sample condensation, then only the GC uncertainty of ±5% applies. If the sample concentrations were altered by condensation, the uncertainty is larger than ±5%. The only arithmetic operations used in this study are sums, differences, and multiplication, so for random errors of small magnitude, the uncertainty can be estimated by addition in quadrature [21]. The uncertainty ε, in a calculated value v is

$$\varepsilon_v = \sqrt{\Sigma \varepsilon_i} \tag{5.13}$$

where ε_i are the fractional uncertainties in terms used to calculate v. In this manner, the uncertainty in the derivatives of the species mass fractions is calculated, as well as the uncertainty in R and $\dot{m}_{OIL}$. The largest uncertainty among the inputs is for $\dot{m}_{OIL}$, which is dependent on the refreshment rate and liner oil mass.

Table 5.3 Uncertainties in model inputs

Term(s)	Explanation	Dependencies	Fractional Uncertainty
M_L	Mass of oil on the liner	cylinder oil volume	± 12.5%
X_{S_i} X_{L_i}	Species mass fractions in oil	GC	± 5%
X_{CC_i}	Species mass fractions in crankcase gas	GC, experimental	≥ ± 5%
$\frac{dX_{S_i}}{dt}, \frac{dX_{L_i}}{dt}$	Time rate of change of species mass fractions in oil	X_{L_i}, X_{S_i}	± 7%
$\frac{dX_{cc_i}}{dt}$	Time rate of change of species mass fractions in crankcase gas	X_{CC_i}	≥ ± 7%
R	Liner oil refreshment rate	$X_{L_i}, X_{S_i}, \frac{dX_{s_i}}{dt}$	± 15%
$\dot{m}_{OIL}$	Oil mass flow rate	R, M_L	± 19%

The model inputs in Table 5.3 were used to calculated the species mass fluxes of interest, $\dot{m}_{SC_i}$, $\dot{m}_{LC_i}$ and $\dot{m}_{net_i}$. All the species mass flux uncertainty estimates are based on the assumption that the uncertainty in the mass of liner oil is ±12.5%. For each species mass flux, the fractional uncertainty is nearly 25%. While this represents substantial uncertainty in the magnitude of the species mass fluxes, the

directions and approximate magnitudes of all the fluxes remain unchanged. For example, $\dot{m}_{SC_i}$, which is the species mass flux from the crankcase gas to the sump oil, has a fractional uncertainty of $\pm 22\%$. For toluene (Fig. 5.10), this means $\dot{m}_{SC_i} / \dot{m}_{\mathrm{inj}_i}$ at 180 minutes is between 1.32% and 0.88%. The calculated uncertainty for $\dot{m}_{LC_i}$ is greater than or equal to 23% because of the uncertainty in X_{CC_i} and the estimates of blow-by flow rate and fraction of charge in blow-by. An example of a calculated species flux with the uncertainty bounds of Table 5.4 is shown in Fig. 5.19.

Table 5.4 Uncertainties in calculated species mass fluxes

Species Mass Flux	Explanation	Dependencies	Fractional Uncertainty
$\dot{m}_{SC_i}$	Crankcase gas to sump oil flux	$X_{L_i}, X_{S_i}, \frac{dX_{S_i}}{dt}, \dot{m}_{OIL}$	$\pm 22\%$
$\dot{m}_{LC_i}$	Crankcase and blow-by gas to liner oil flux	$\frac{dX_{CC_i}}{dt}, \dot{m}_{SC_i}$, others	$\geq \pm 23\%$
$\dot{m}_{net_i}$	$\dot{m}_{LC_i}$ and $\dot{m}_{abs_i}$	$X_{L_i}, X_{S_i}, M_L, \frac{dX_{L_i}}{dt}, \dot{m}_{OIL}$	$\pm 25\%$

5.13 Conclusions

In this chapter, a framework for the mass transport of fuel species between the crankcase gas, sump oil and liner oil was presented. In order to calculate species mass fluxes of interest, several parameters needed to construct a fuel transport model were calculated. The liner oil refreshment rate was estimated from experimental data, as was the concentration of fuel species in blow-by gas. Species balances involving the mass fluxes interacting with the engine oil and crankcase gas were applied to appropriate control volumes to obtain mass fluxes. The control volumes established were the liner oil, sump oil and crankcase gas. The species mass fluxes between the crankcase gas and sump oil were determined, as were the mass fluxes between the liner oil and both the crankcase and blow-by gas. The mass fluxes describing the net interaction of the liner oil layer with the mechanisms of liquid fuel impingement, and absorption and desorption to cylinder, crankcase, and blow-by gases were also calculated. These mass fluxes were determined during warm-up conditions and up to 180 minutes of operation. Five fuel species which span the molecular weight range of the test fuel were chosen as model inputs, along with the total fuel concentration in oil. The fuel concentrations were obtained from the oil sampling and analysis described in previous chapters.

The calculations described in this chapter show that there are species mass fluxes from the crankcase gas to the sump oil which increase with engine operating time, until steady state concentrations of

fuel in oil are reached. These mass fluxes are generally larger in magnitude for higher molecular weight fuel species and varied from 0% to 14% of the rate at which individual fuel species are injected into the cylinder during stoichiometric operation. From calculations involving the mass fluxes interacting with the liner oil layer, it was determined that for each of the species modeled during warm-up, there is a net flux of fuel species to the liner oil from cylinder, crankcase and blow-by gas fuel species as well as possibly liquid fuel species impinging on the liner. The direction of this mass flux reverses at the point when the concentration of fuel in the liner oil is equal to that in the sump oil. Using crankcase gas data of 2-methylpentane and toluene, the mass fluxes between the liner oil and both the crankcase and blow-by gas were calculated. For 2-methylpentane after 20 minutes, the direction of fuel transport was from the liner oil layer to the crankcase gas and blow-by gas, with a magnitude of nearly 1% of the stoichiometric rate of 2-methylpentane injection. For toluene, the calculated direction of species transport was from the crankcase gases and blow-by to the liner oil layer, with approximately 0.6% of the rate of injected toluene transported in this manner. In addition, for steady state, the amount of toluene desorbing to the cylinder gas was calculated to be 0.6% of the rate of injected toluene. It is evident from examining different classes of fuel species, that the liner oil is a source of light hydrocarbons to the crankcase gases and blow-by, while the sump oil is a sink for the heavy fuel species.

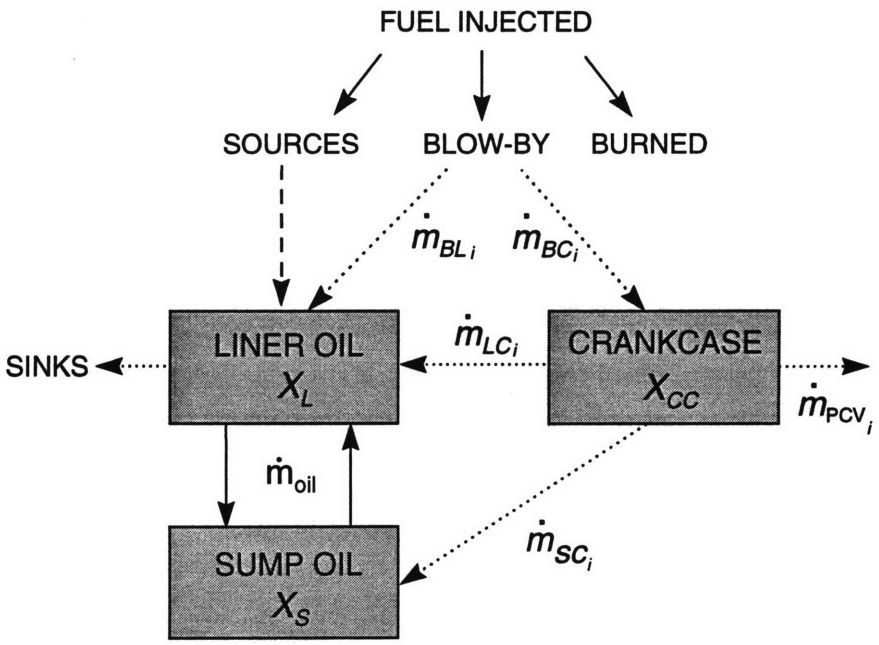

Fig. 5.1 Framework for fuel transport in engine oil. Italicized symbols are mass fluxes of fuel species. Dashed lines represent fuel transport in the gas phase between shaded control volumes, and solid lines indicate transport by oil. The mass flux $\dot{m}_{PCV_i}$ is recycled to the intake manifold.

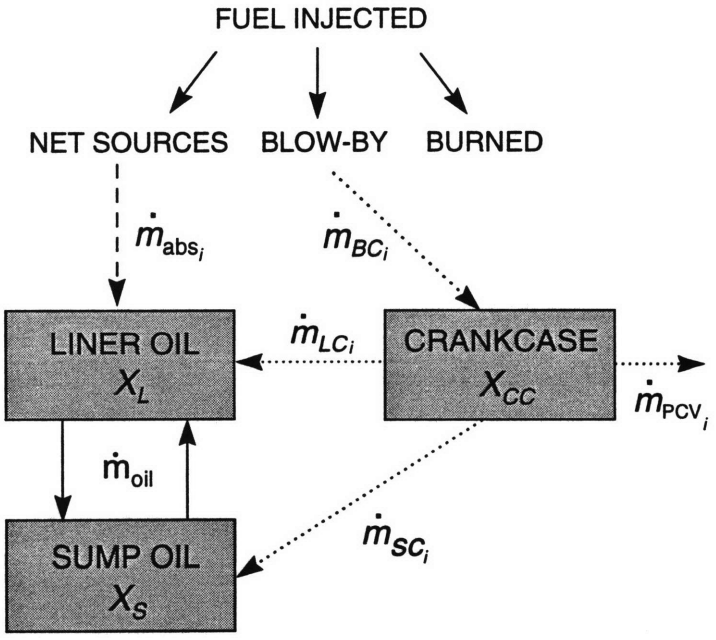

Fig. 5.2 Simplified fuel transport framework. Note particularly the change in how blow-by gas exchange is modeled.

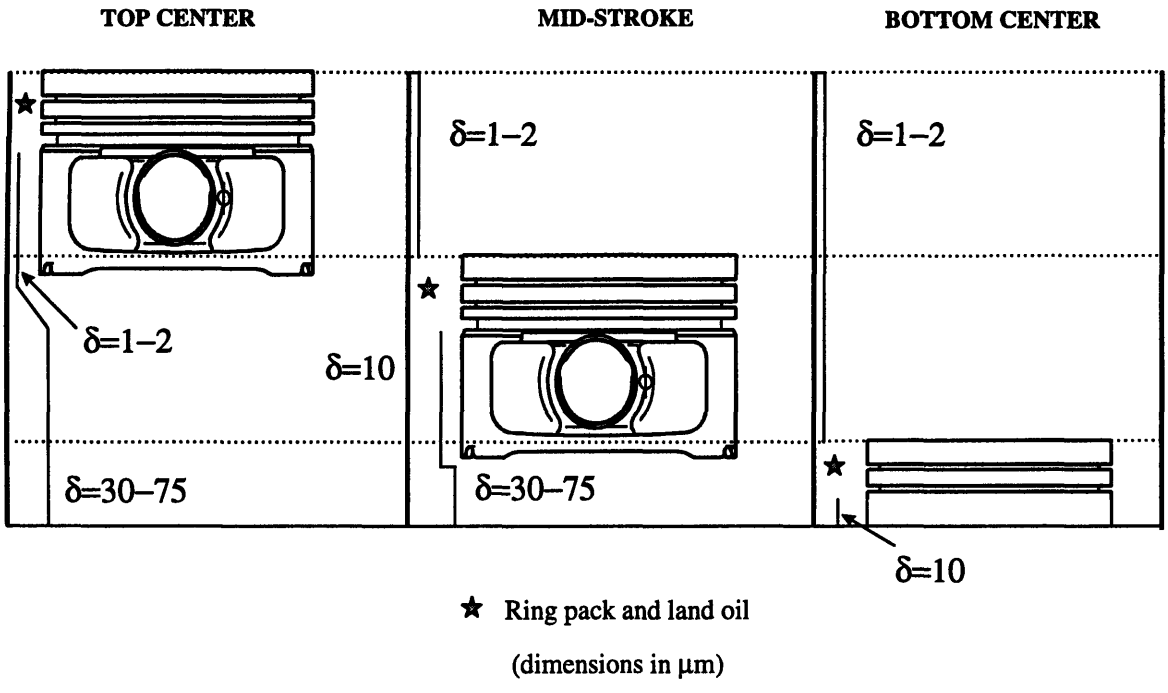

Fig. 5.3 Estimated oil film thickness on the liner for different piston positions.

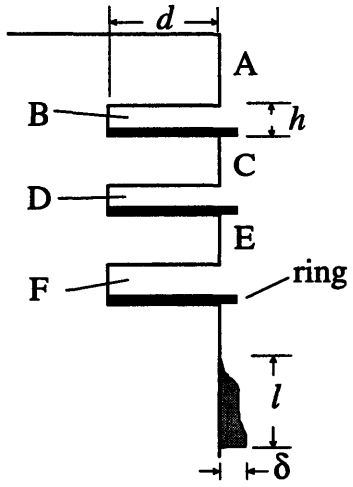

Location	Approximate OFT or Groove State	Approximate Volume (cm^3)
A. Top Land	1 μm	1.0E-03
B. Pressure Ring Groove	10% flooded	0.04
C. Second Land	5 μm	4.4E-03
D. Scraper Ring Groove	20% flooded	0.10
E. Third Land	10 μm	7.6E-03
F. Oil Control Ring Groove	Fully Flooded	0.92

Fig. 5.4 Estimated oil film thickness on piston lands and volume of oil in ring grooves.

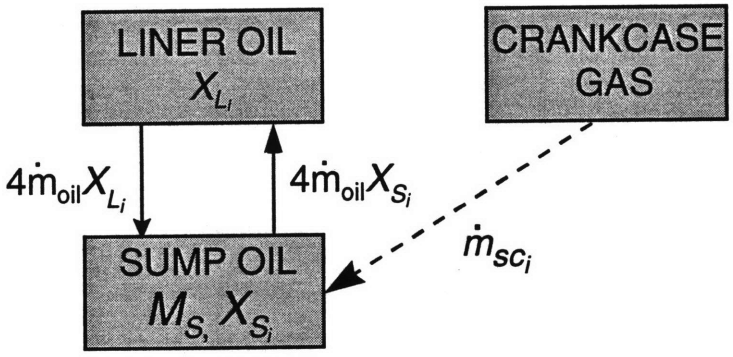

Fig. 5.5 Sump oil control volume with interacting species fluxes. X_{L_i} and X_{S_i} are the mass fractions of fuel species i in the liner and sump oil, respectively. M_L and M_S are the masses of the liner oil and sump oil. The crankcase to sump mass species flux is $\dot{m}_{SC_i}$, and the mass flow rate of oil between the liner and sump is $\dot{m}_{oil}$.

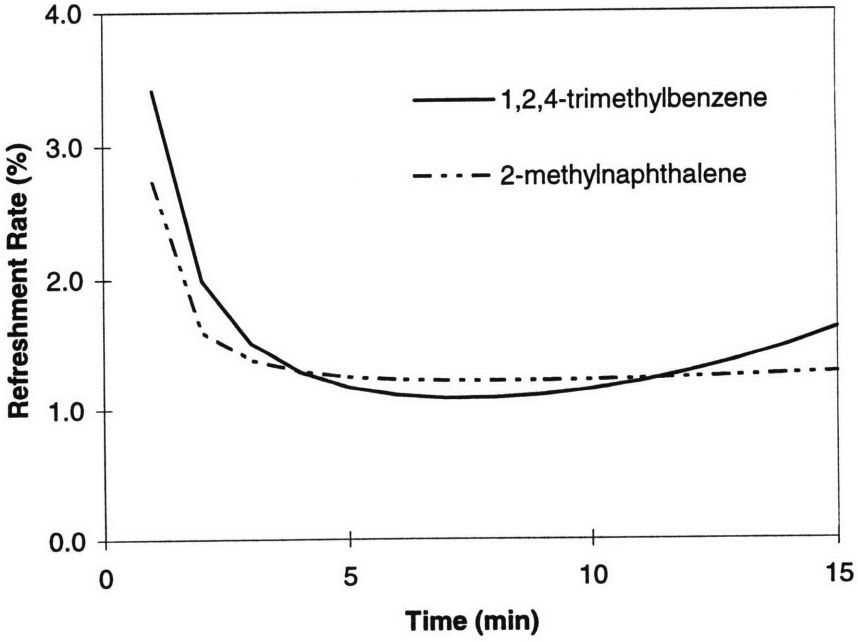

Fig. 5.6 Calculated results for the oil refreshment rate.

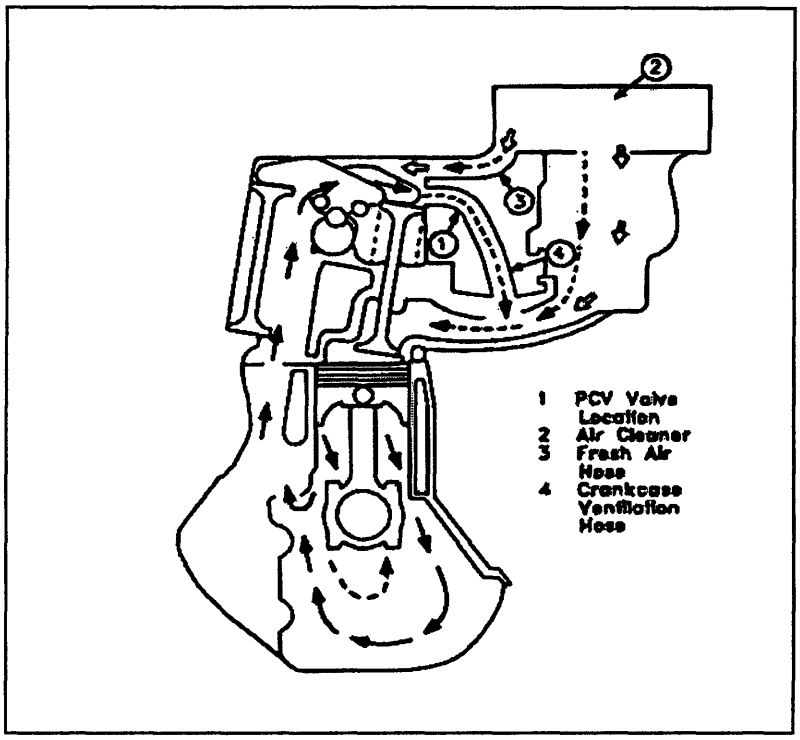

Fig. 5.7 Positive crankcase ventilation system in the Saturn 1.9 L engine. The fresh air hose marked '3' is sealed in the test engine. Blow-by past the piston rings is shown, as is the route by which $\dot{m}_{PCV_i}$ enters the intake manifold at '1' *(Saturn engine manual)*.

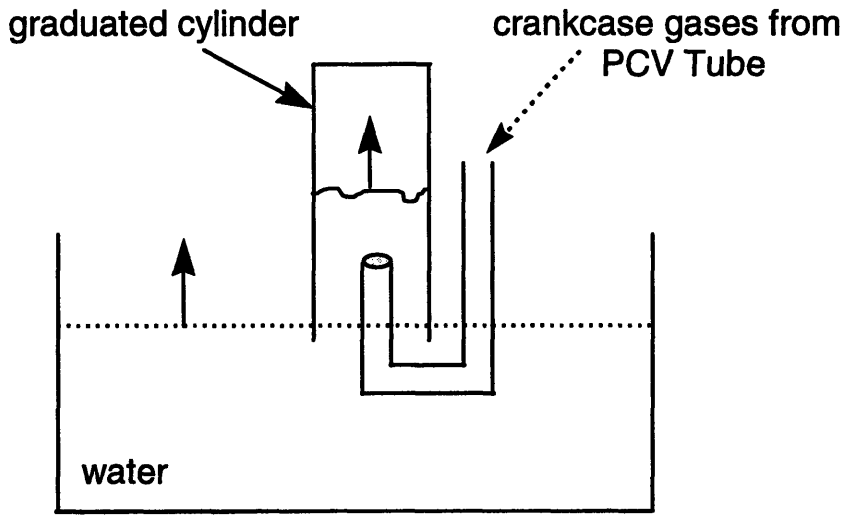

Fig. 5.8 Schematic of experimental setup to measure blow-by gas flow rate.

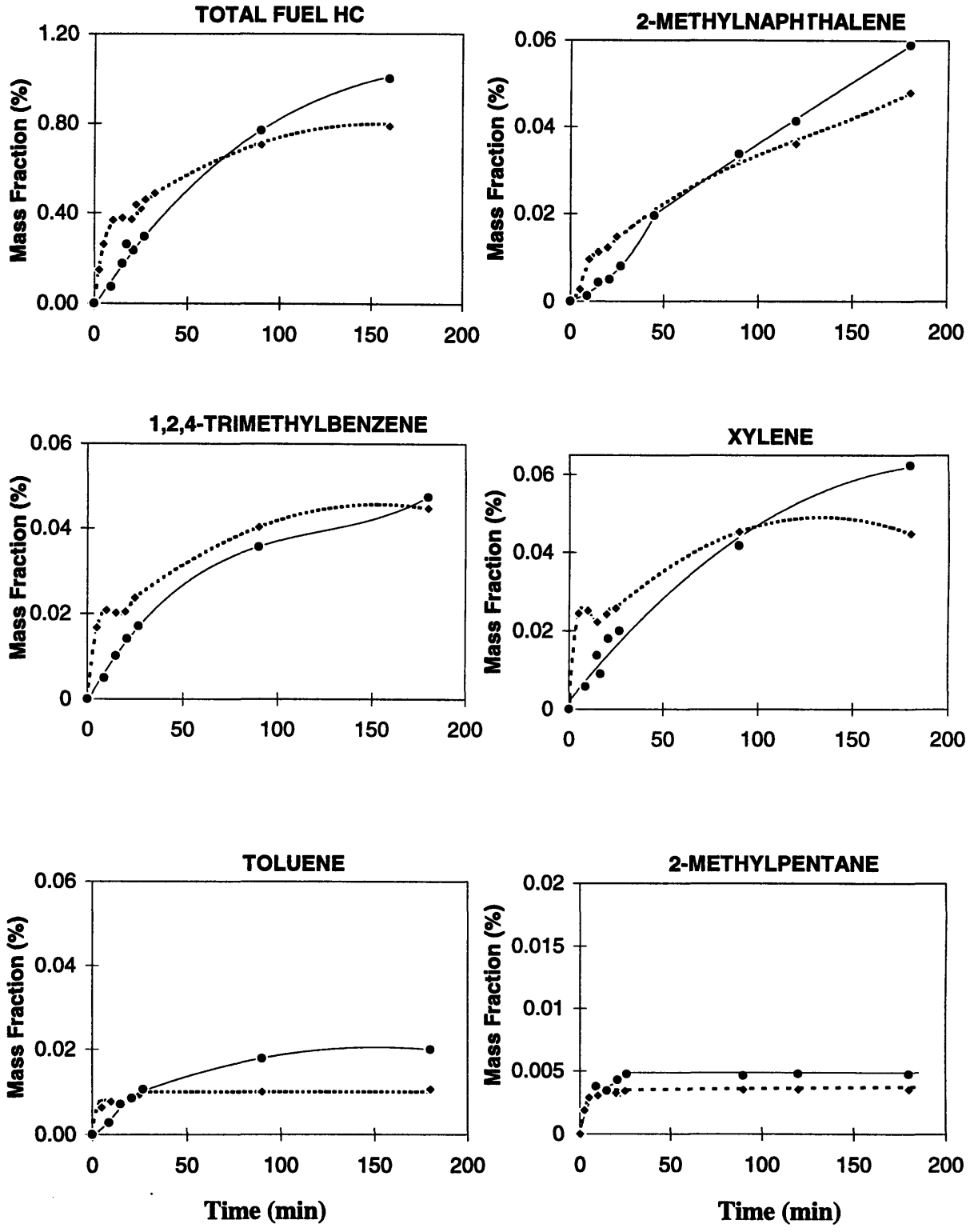

Fig. 5.9 Polynomial curve fits of the mass fraction of fuel species in the liner (dashed lines) and sump oil (solid lines). Note the difference in scale for the total fuel HC and 2-methylpentane.

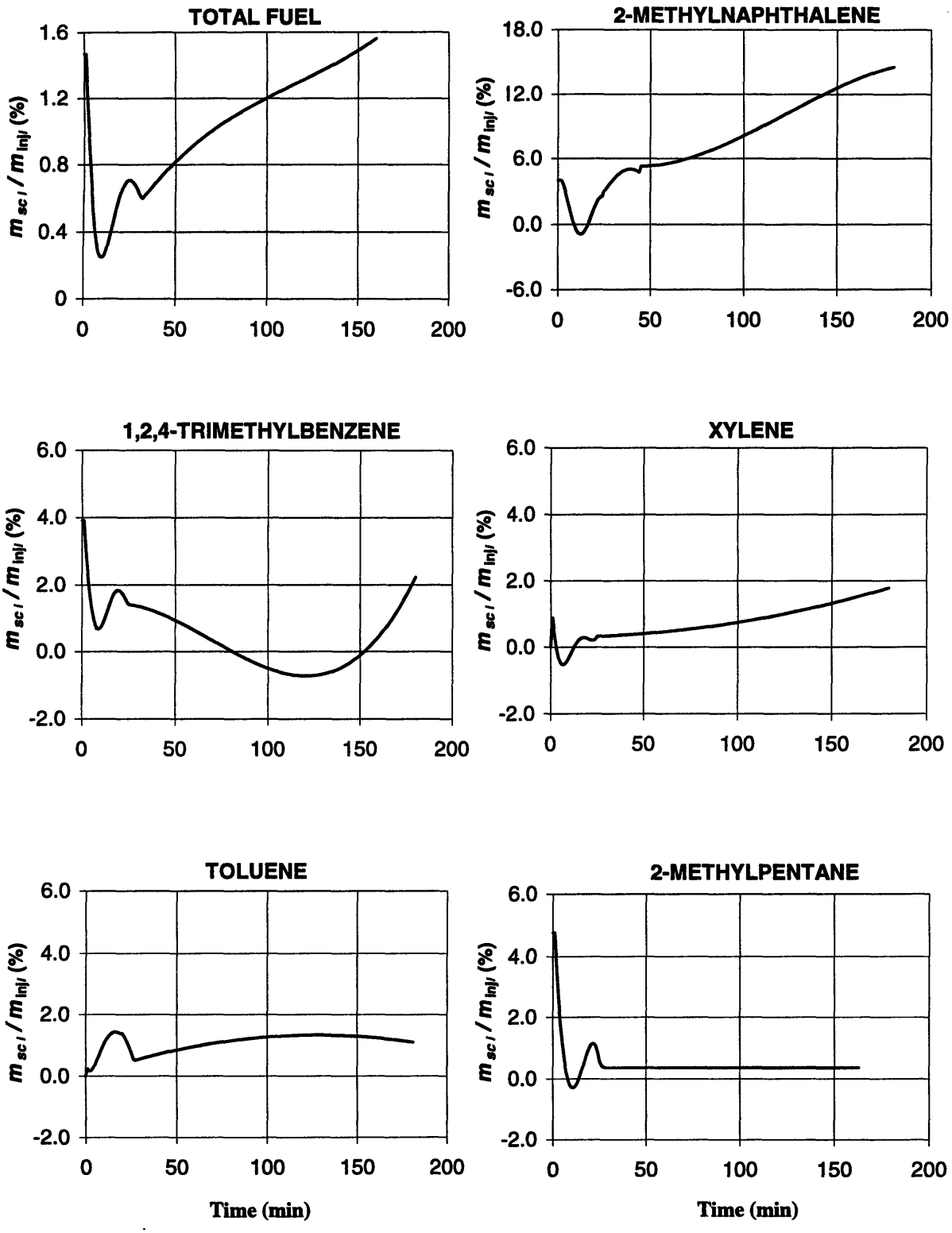

Fig. 5.10 Calculated crankcase gas to sump oil species mass flux $\dot{m}_{SC_i}$, normalized by the rate each fuel species is injected into the engine during stoichiometric operation. A positive $\dot{m}_{SC_i} / \dot{m}_{\text{inj}_i}$ indicates fuel species mass transport to the sump oil.

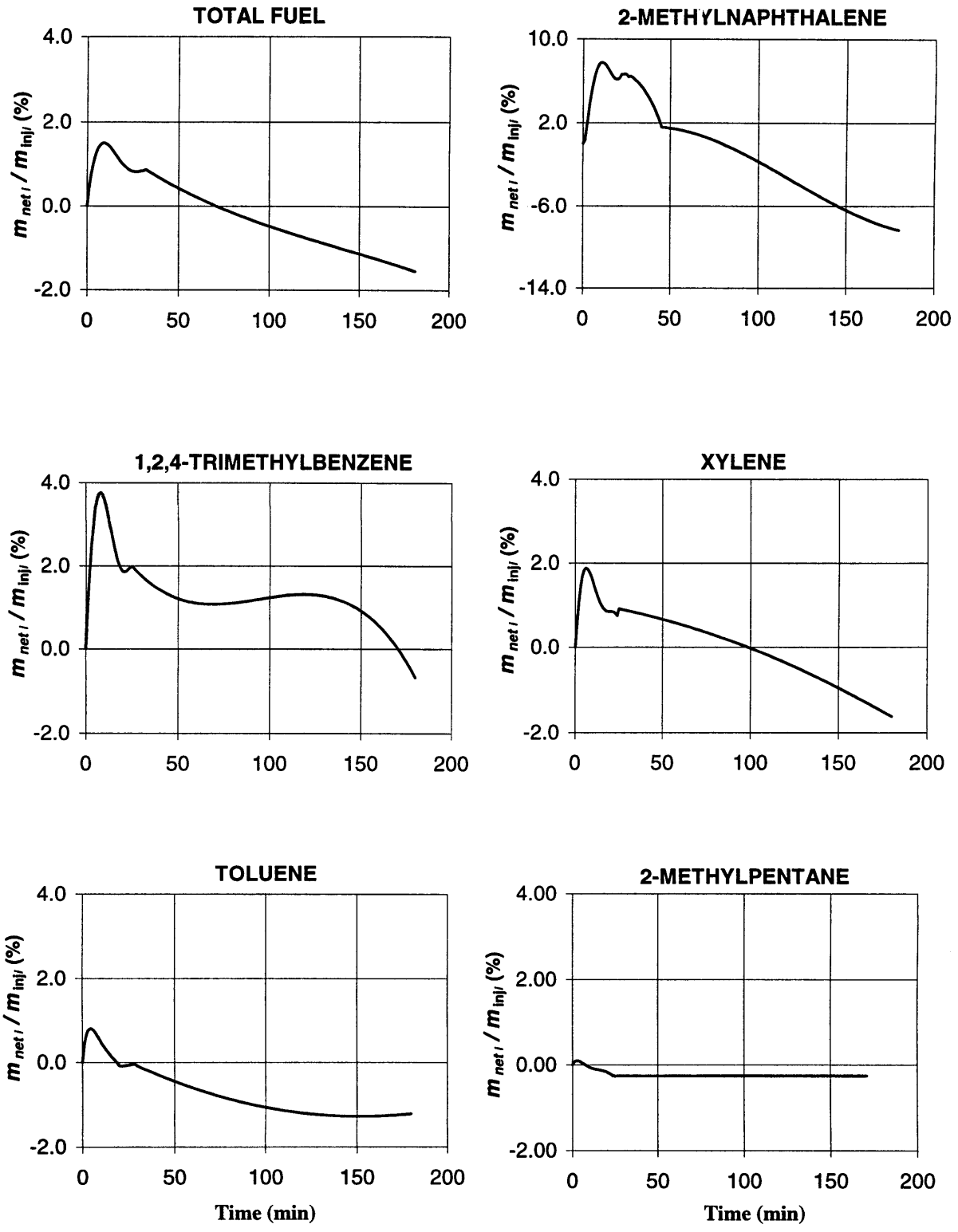

Fig. 5.11 Calculated liner oil fuel species mass flux $\dot{m}_{net\,i}$ normalized by the rate each fuel species is injected into the engine during stoichiometric operation. A positive $\dot{m}_{net\,i} / \dot{m}_{inj_i}$ indicates fuel species mass transport to the liner oil.

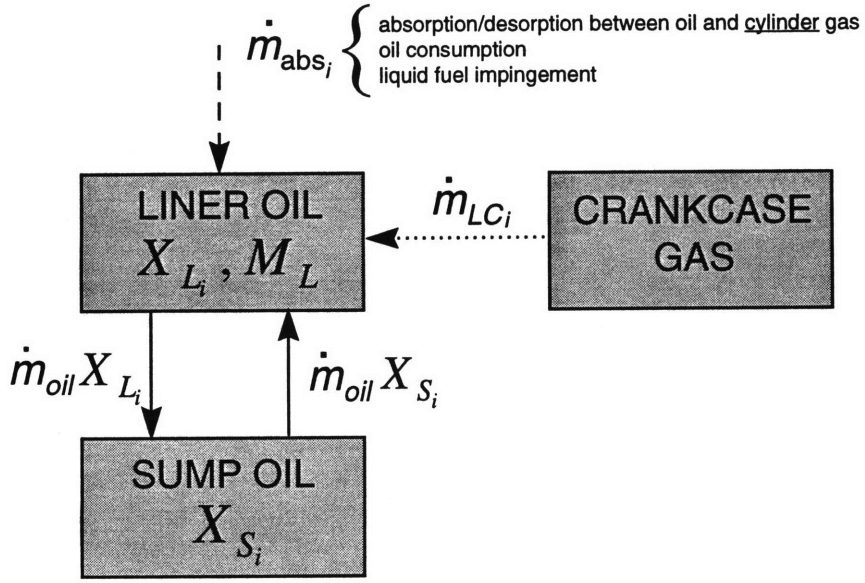

Fig. 5.12 Liner oil control volume with interacting species mass fluxes.

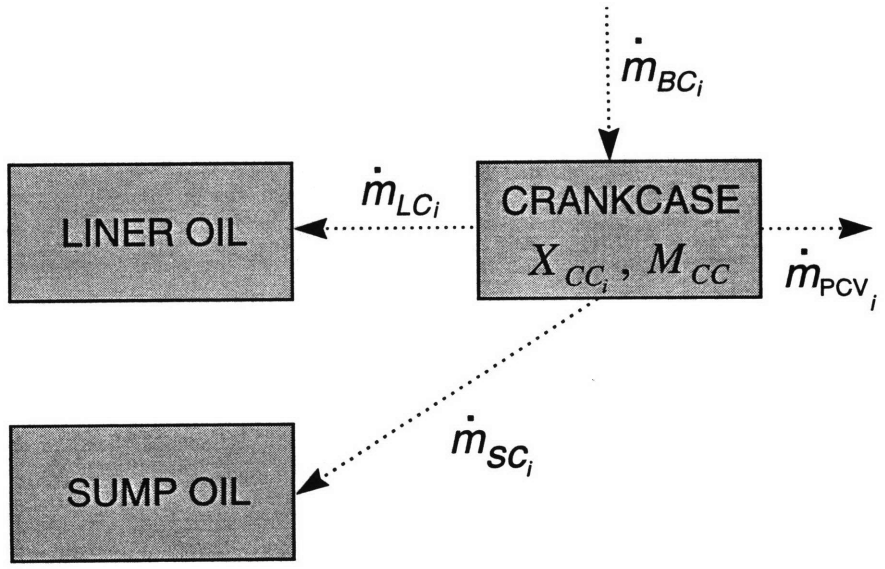

Fig. 5.13 Crankcase gas control volume with interacting species mass fluxes.

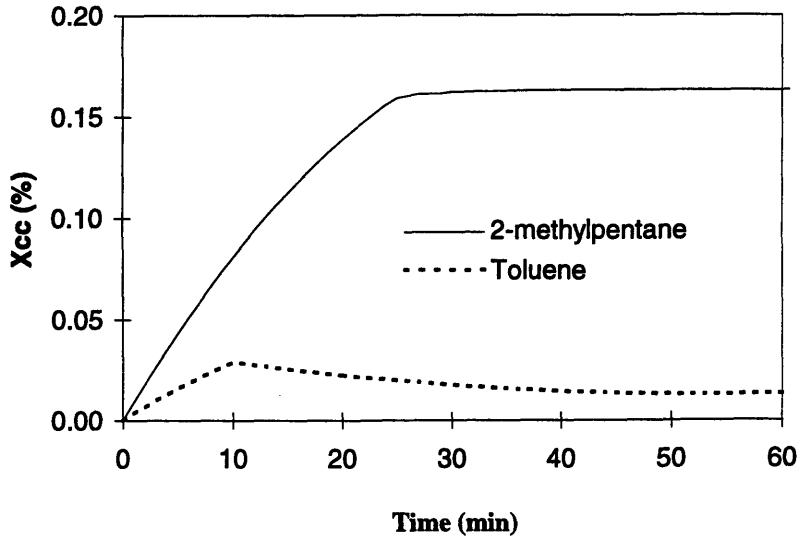

Fig. 5.14 Curve fit of the crankcase gas mass fractions of toluene and 2-methylpentane.

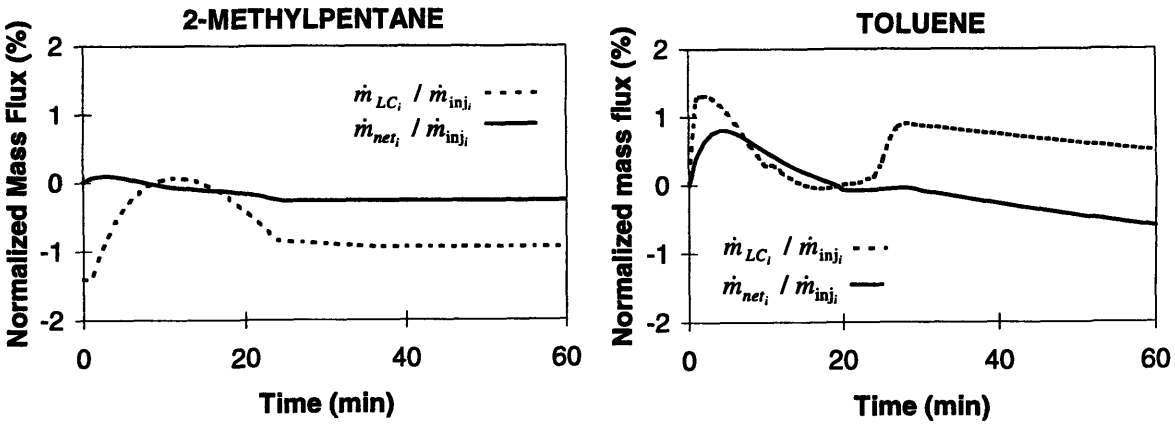

Fig. 5.15 Calculated values $\dot{m}_{LC_i} / \dot{m}_{inj_i}$ and $\dot{m}_{net_i} / \dot{m}_{inj_i}$ for toluene and 2-methylpentane. Positive values indicates fuel species mass transport to the liner oil.

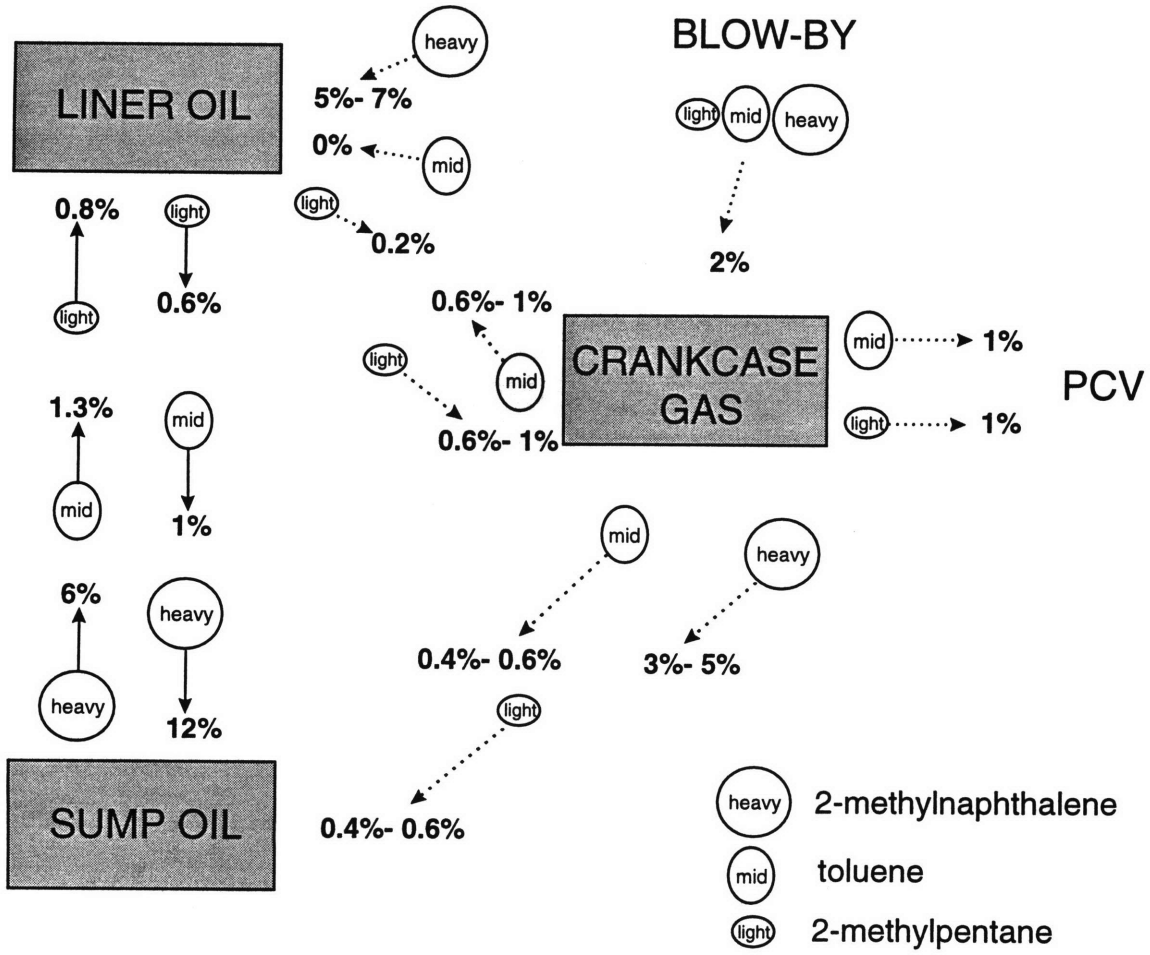

Fig. 5.16 Species mass fluxes for light, intermediate, and heavy fuel species at the end of warm-up (30 minutes). The percentages shown are species fluxes normalized by the rate of injection of each fuel species during stoichiometric engine operation. The range in value for a particular species flux corresponds to the likely uncertainty in a species flux. The species flux to the right of the liner oil is the net (non-oil) fuel species transport to the liner oil. The species flux to the left of the crankcase gas is the species flux between the liner oil layer and both the crankcase gas and blow-by gas.

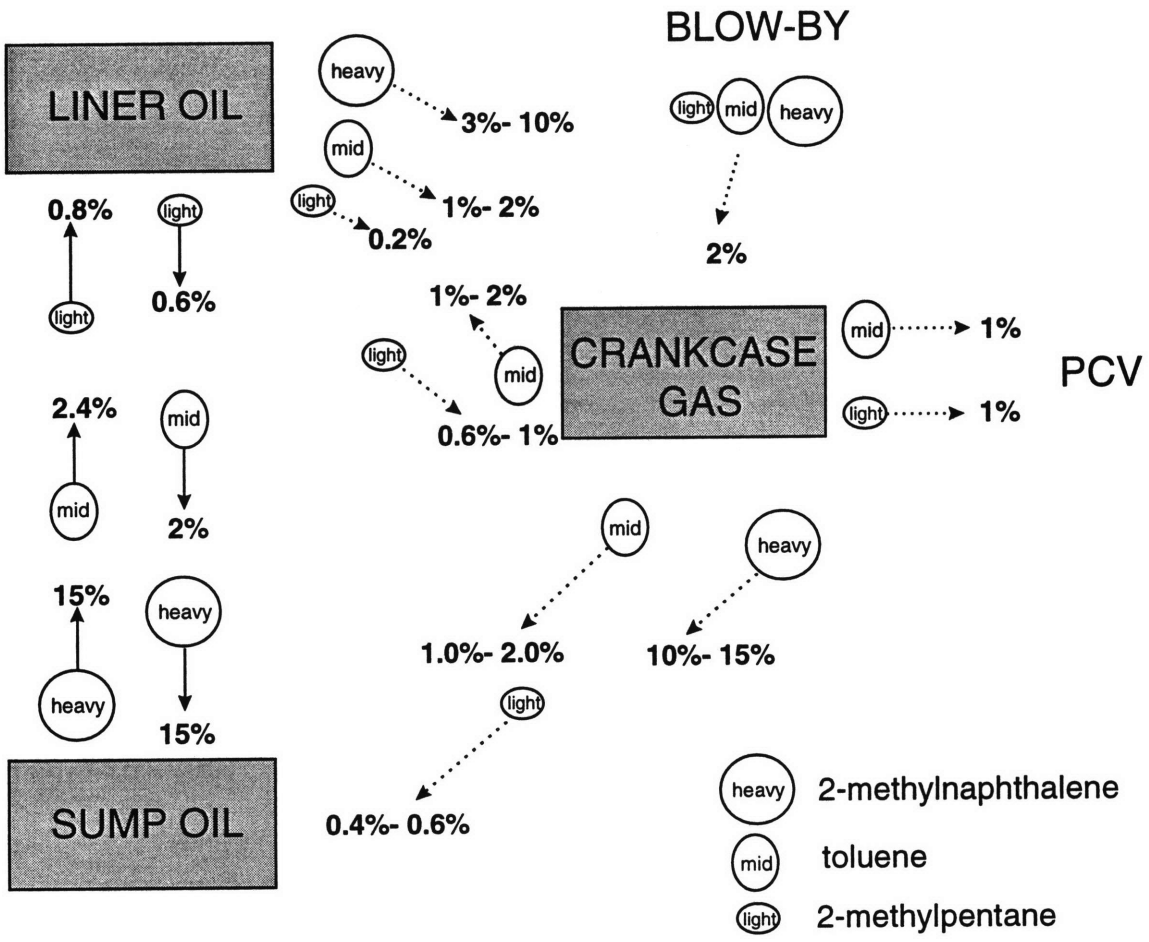

Fig. 5.17 Species mass fluxes for light, intermediate, and heavy fuel species after 3 hours. The percentages shown are species fluxes normalized by the rate of injection of each fuel species during stoichiometric engine operation. The range in value for a particular species flux corresponds to the likely uncertainty in a species flux. The species flux to the right of the liner oil is the net (non-oil) fuel species transport to the liner oil. The species flux to the left of the crankcase gas is the species flux between the liner oil layer and both the crankcase gas and blow-by gas.

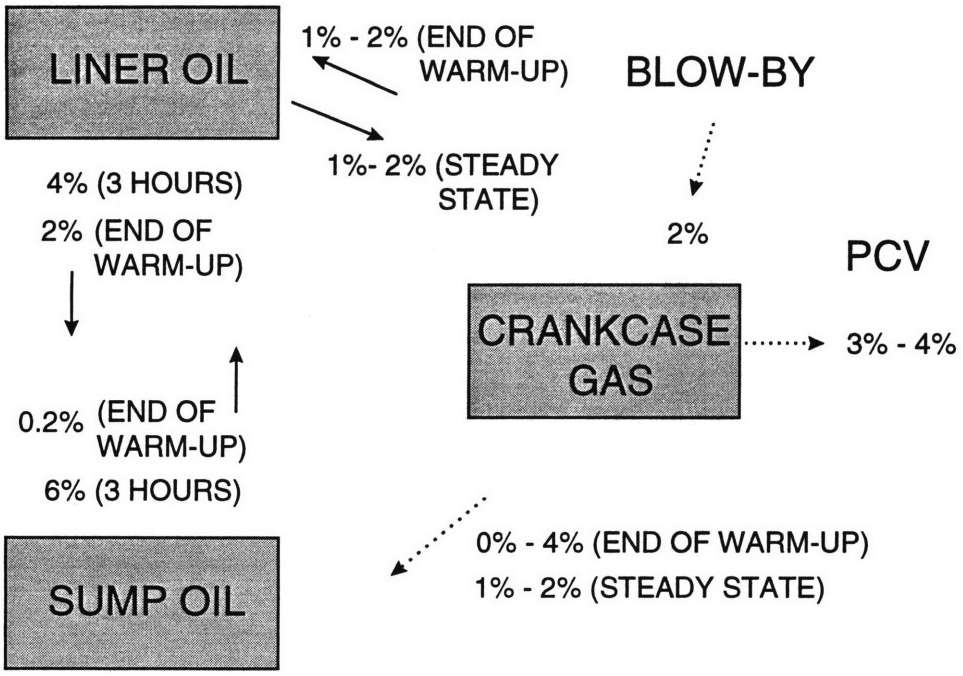

Fig. 5.18 Species mass flux for the total fuel at the end of warm-up and after three hours. The percentages shown are mass fluxes normalized by the rate that fuel is injected during stoichiometric engine operation. A description of some of the mass fluxes is in Fig. 5.17.

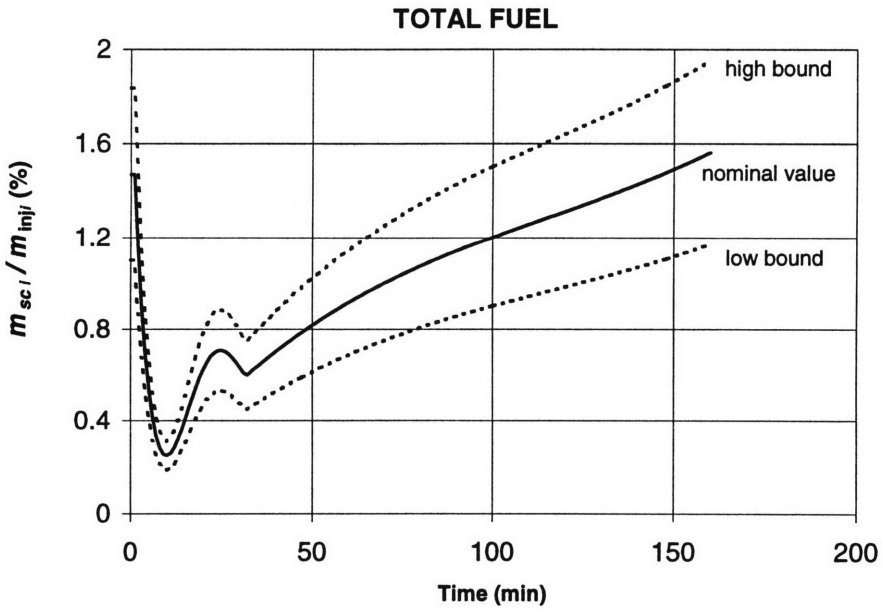

Fig. 5.19 Example of a calculated species flux with uncertainty bounds.

CHAPTER 6

SUMMARY AND CONCLUSIONS

In this study, an experimental method was used to obtain the liner oil and sump oil from a firing spark-ignition engine operating at a part-load, low speed condition. Liner oil samples were obtained from the thrust and anti-thrust side of the piston skirt for both cold start and steady state conditions. Oil sampling from 0.5 mm below the oil control ring groove on the piston skirt yielded sufficient quantities of sampled oil for analysis. The sampling flow-rates from the piston skirt were sufficiently high to obtain samples within five minute intervals, and lubrication of the liner was not altered using this method. The oil samples were analyzed using an adapted gas chromatography method enabling fuel species to be identified and quantified for the duration of the experimental tests.

In experiments using a standard fuel and lubricant, the mass fraction of fuel in the liner oil rises at a rate nearly four times faster than that in the sump oil, during the first ten minutes of engine warm-up. The fuel build-up rate in the liner oil matches the change in calculated liner oil temperature. At the conclusion of engine warm-up, the mass fraction of fuel in the liner oil for the experimental conditions is 0.41% and 0.29% in the sump oil. After three hours of engine operation, the fuel mass fraction in the sump oil is 1.04%, compared to 0.78% in the liner oil. A crossover point, when the fuel concentration in the sump oil exceeds fuel concentration in the liner oil, occurs at approximately 70 minutes for the conditions of this study. The crossover point indicates that there is another source of fuel to the sump oil, since increasing concentrations in the sump oil cannot be explained by oil transport from the liner.

Heavy hydrocarbons are preferentially absorbed in both the liner and sump oil, and the differences in absorption between fuel species do not scale with the relative amount of each species in the fuel. Lighter hydrocarbons reach the concentration crossover point and steady state during engine warm-up. There is a steady state concentration of all fuel species in the liner oil after two hours of engine operation, but heavy species are still absorbing into the sump oil after three hours. Correspondingly, the concentration crossover points occur at times greater than two hours for the heaviest fuel species. For the heaviest fuel species, up to 4.5% of the total amount injected is present in the sump oil after three hours of engine operation. Oil sampled from opposite sides of the piston skirt has identical fuel concentrations relative to the sump oil. At steady state, a strong correlation was observed between the mass fraction of fuel species absorbed and individual boiling points, in both the liner and sump oil. This indicates that for increasing fuel species volatility, a decreasing amount of fuel species are absorbed into engine oil. Fuel variation tests indicate that the solubility and volatility of fuel species may be separate factors in the fuel absorption process.

A description of the mass transport of fuel species between the crankcase gas, sump oil, and liner oil of the test engine was developed in this study. Equations involving the species mass fluxes which

interact with engine oil and crankcase gas were formulated by applying mass conservation to species within appropriate control volumes. The liner oil, sump oil and crankcase gas were defined as three control volumes of interest. Five fuel species which span the molecular weight range of the test fuel were chosen as model inputs, along with the total fuel concentration in oil. The fuel concentrations used as an input to the calculations were obtained from the oil sampling experiments of this study. Other input parameters, such as the liner oil refreshment rate and mass fraction of fuel in blow-by gas, were obtained through experiment and analysis.

Calculations indicate the presence of a species mass flux from the crankcase gas to the sump oil which increases with engine operating time, until steady state concentrations of fuel in oil are reached. The magnitude of this species flux is generally larger for higher molecular weight fuel species, and varies from 0% to 14% of the fuel species injection rate during stoichiometric operation. From calculations involving the liner oil control volume, it was determined that during engine warm-up, there is a net flux of fuel species to the liner oil from cylinder, crankcase and blow-by gas fuel species. The direction of this mass flux reverses at the point where the concentration of fuel in the liner oil is equal to that in the sump oil. For light fuel species, the mass flux between the liner oil and both the crankcase and blow-by gas was calculated. After warm-up, the calculated direction of toluene mass transport was from the crankcase gas and blow-by gas to the liner oil layer. The direction of 2-methylpentane transport following warm-up was opposite that of toluene. For the light fuel species, there is a net mass flux from the liner oil and for heavy fuel species, the sump is a fuel species sink. Uncertainty in the model calculations was estimated, and while there is moderate uncertainty in the magnitude of the calculated species mass fluxes, their direction is not affected by this uncertainty.

REFERENCES

[1] Jimenez, J.L., "Introduction to Mobile Source Emissions," Lecture, Massachusetts Institute of Technology, February 24, 1997

[2] Cheng, W.K., Hamrin, D., Heywood, J.B., Hochgreb, S., Min, K., Norris, M., "An Overview of Hydrocarbon Emissions Mechanisms in Spark-Ignition Engines," *SAE Paper No. 932708* (1993)

[3] "Emissions Standards-Passenger Cars Worldwide," Delphi Technical Centre Publication, Luxembourg, September (1995)

[4] Heywood, J.B., Internal Combustion Engine Fundamentals, McGRaw Hill, Inc., New York, pp. 604-608, 146-148, 364 (1988)

[5] Takeda, K., Yaegashi, T., Sekiguchi, K., Saito, K., and Imatake, N., "Mixture Preparation and HC Emissions of a 4-Valve Engine with Port Fuel Injection During Cold Starting and Warm-up," *SAE Paper No. 950074* (1995)

[6] Alkidas, A.C., Drews, R.J., "Effects of Mixture Preparation on HC Emissions of a S.I. Engine Operating Under Steady-State Cold Conditions,"

[7] Ishizawa, S., and Takagi, Y., "A Study of HC Emissions from a Spark-Ignition Engine," JSME Int. J., Vol. 30, No. 260 (1987)

[8] Norris, M.G., "Oxidation of Hydrocarbons Desorbed from the Lubricant Oil in Spark Ignition Engines," PhD Thesis, Massachusetts Institute of Technology (1995)

[9] Schwartz, S.E., "Observations Through a Transparent Oil Pan During Cold-Start, Short Trip Service," *SAE Paper 912387* (1991)

[10] Murakami, Y., and Aihara, H., "Analysis of Mechanism Intermixing Combustion Products in Engine Oil (Quantity and Composition of Unburned Gasoline in Engine Oil and Crankcase Gas)," JSME Int. J., Series II, Vol. 34, No 4 (1991)

[11] Saville, S.B., Gainey, F.D., Cupples, S.D., Fox, M.F., and Picken, D.J., "A Study of Lubricant Condition in the Piston Ring Zone of Single-Cylinder Diesel Engines Under Typical Operating Conditions," *SAE Paper No. 881586* (1988)

[12] Frottier, V., Heywood, J.B., Hochgreb, S., "Measurement of Gasoline Absorption into Engine Lubricating Oil", *SAE Paper 961229* (1996)

[13] "GC Inlets-An Introduction," Hewlett-Packard Part No. 5958-9468

[14] Grob, R.L., Modern Practice of Gas Chromatography, John Wiley and Sons, New York, pp. 413-416 (1985)

[15] Froelund, K., Schramm, J., "Simulation of HC-Emissions from SI Engines During Steady-State and Warm-Up", *SAE Draft Paper*, Submitted for the Fall 1997 Fuels & Lubricants Meeting and Exposition

[16] Linna, J.R., "Personal Correspondence," Massachusetts Institute of Technology (1996)

[17] Jensen, T.E., Siegel, W.O., Richert, R.F.O., Loo, J.F., Prostak, A., Lipari, F., and Sigsby, J.E., "Advanced Emission Speciation Methodologies for the Auto/Oil Air Quality Improvement Research Program - 1. Hydrocarbons and Ethers," *SAE Paper 920320* (1992)

[18] Kayes, D.J., "Crank Angle and Space Resolved, Speciated Sampling of Engine-Out Exhaust Hydrocarbons," MSME Thesis, Massachusetts Institute of Technology (1996)

[19] Tamai, G., "Experimental Study of Engine Oil Film Thickness Dependence on Liner Location, Oil Properties and Operating Conditions," MSME Thesis, Massachusetts Institute of Technology (1995)

[20] Tian, T., Casey, S.M., "Personal Correspondence," Massachusetts Institute of Technology (1996)

[21] Taylor, J.R., An Introduction to Error Analysis, The Study of Uncertainties in Physical Measurements, University Science Books, Mill Valley, California (1982)

[22] Reilly, D. J., Anderson, R. P. Casparian, R. J., and Dugdale, P.H., "Saturn DOHC and SOHC Four Cylinder Engines," *SAE Paper 910676* (1991)

APPENDIX A

OIL SAMPLING EQUIPMENT AND ENGINE SPECIFICATIONS

Table A.1 Oil Sampling Equipment

Part	Specifications	Manufacturer
stainless steel capillary tube (piston skirt to transfer line)	1 mm ID, 1.5 mm OD, 9 mm length	VWR Scientific
PTFE spaghetti tubing (capillary tube to sampling line)	1.2 mm ID, 1.5 mm OD, 101 mm length	Viton
PEEK HPLC tubing (transfer line to pump)	0.762 mm ID, 305 mm length	Jones Chromatography
flow restrictors and tube unions	vary	Manostat Tubing
short form sampling vials	1.5 ml	VWR Scientific
J120 cassette pump Cat. No. 72-510-000	N/A	Manostat
Epoxi-Patch	2.8 oz	Dexter Corporation

Table A.2 Saturn Engine Specifications

Specification	Value
No. of cylinders, valves/cylinder	4,4
Bore x Stroke (mm)	82 x 90
Displacement (cc), Valvetrain	1901, DOHC
Compression Ratio, Combustion Chamber	9.5:1, pent roof
Fuel System	Port fuel injection (Closed Valve)
Max Power (SAE kw @ RPM)	92.5 @ 6,000
Max Torque (SAE N-m @ RPM)	165 @ 4,800

APPENDIX B

GAS CHROMATOGRAPHY AND FUEL SPECIFICATIONS

B1. Analytical Method to separate gasoline components in lubricant oil

(see also 'Frottier, V, Heywood, J.B., Hochgreb, S., "Measurement of Gasoline Absorption into Engine Lubricating Oil", *SAE Paper 932708* (1993))

Table B1. Gas flow rates for the Hewlett-Packard 5890 gas chromatograph

Flow	Cylinder Gas (grade)	Rate (ml/min)	Measuring location
column	helium (4.7) / 22 psi column head	3	detector outlet
septum purge	helium (4.7)	3	purge vent
split (split ratio- 3:30)	helium (4.7)	30	total flow outlet
auxilliary gas	nitrogen (4.8)	7	detector outlet
FID fuel	hydrogen (4.7)	25	detector outlet
Oxidizer	air (dry grade)	260-270	detector outlet

Temperature Information

Inlet temperature: 200 °C

Detector temperature: 300 °C

Initial oven temperature: 35 °C

Table B2. Oven temperature program for fuel analysis in oil

	Rate (C/min)	Final Temp (°C)	Final Time (min)
Level 1	0.1	35	10.0
Level 2	2	183	0.0
Level 3 - column maintenance	20	300	60

Table B3. Integration events in Hewlett-Packard Chemstation analysis software

Event	Value
Initial Area Reject	1
Initial Peak Width	0.040
Shoulder detection	OFF
Inital Threshold	0

Table B4. Major fuel species in Chevron FR1760 reference fuel

Fuel Component	Number of carbon atoms	Mass Fraction of component in Chevron fuel (%)
butane	4	4.54
2-methylpropane	4	1.03
2-methylbutane	5	6.31
pentane	5	2.47
MTBE	6	9.69
methylcyclopentane	6	2.30
benzene	6	1.24
2-methyhexane	7	1.53
toluene	7	4.94
xylenes (m, p, and o)	8	6.37
ethylbenzene	8	1.14
1,2,4-trimethylbenzene	9	2.37
Naphthalene	10	0.57
2-methylnaphthalene	11	0.74